ISTITUTO DI ANALISI DEI SISTEMI ED INFORMATICA
"Antonio Ruberti"
CONSIGLIO NAZIONALE DELLE RICERCHE

C. Bruni, F. Conte, F. Papa, C. Sinisgalli

Optimal number and sizes of the doses in fractionated radiotherapy

R. 06, 2016

Bruni – Dipartimento di Ingegneria Informatica, Automatica e Gestionale "A. Ruberti" — Via Ariosto 25 — 00185 Roma, Italy (brunic@dis.uniroma1.it).

Conte – Istituto di Analisi dei Sistemi ed Informatica 'A. Ruberti' - CNR, Sapienza Università di Roma — Via dei Taurini 19 — 00185 Roma, Italy (conte@dis.uniroma1.it).

Papa – Istituto di Analisi dei Sistemi ed Informatica 'A. Ruberti' - CNR, Sapienza Università di Roma — Via dei Taurini 19 — 00185 Roma, Italy (federico.papa@iasi.cnr.it).

Sinisgalli – Istituto di Analisi dei Sistemi ed Informatica 'A. Ruberti' - CNR — Via dei Taurini 19 — 00185 Roma, Italy (carmela.sinisgalli@iasi.cnr.it).

ISSN: 1128–3378

Collana dei Rapporti dell'Istituto di Analisi dei Sistemi ed Informatica "Antonio Ruberti", CNR

via dei Taurini 19, 00185 ROMA, Italy

tel. ++39-06-49937101/02
fax ++39-06-49937106
email: iasi@iasi.cnr.it
URL: http://www.iasi.cnr.it

Abstract

We address the problem of finding the optimal dose fractionation for cancer radiotherapy schedules of the kind one fraction/day, five fractions/week. Using the LQ model with exponential repopulation to represent the radiation response of tumour and normal tissues, we formulate a constrained nonlinear programming optimization problem in terms of the dose fraction sizes and of the total number of dose fractions. Constraints are imposed to guarantee that the damages to the early and late reacting normal tissues do not exceed maximal tolerable levels, as well as to limit the size of the daily dose fractions. The optimal solutions are found in two consecutive steps. The first step is the analytical determination of the optimal dose sizes for a fixed, but arbitrary number of fractions. The optimal protocols are classified according to the values of the tumour radiosensitivity ratio, α/β, and of the daily dose upper bound, while the optimal fraction sizes are expressed as a function of the normal tissue parameters. The second step of the optimization consists in the numerical computation of the optimal number of dose fractions, and then of the optimal overall treatment time, considering specific tumour classes identified by the values of α/β. We prove that the optimal number of fractions is finite so that it can be determined by a limited number of direct comparisons among the cost function values obtained for the sequence of optima with fixed length. While the radiosensitivity and repopulation parameters of the early and late responding tissues are set according to the literature, we investigate the behaviour of the optimal solution, even in comparison with standard clinical protocols, for wide variations of the tumour parameters and of the daily dose upper bound, evidencing the influence of the model parameters on the optima. In particular, we recognize that the value of the tumour α/β ratio compared to the the normal tissue radiosensitivity determines the hypo- or equi-fractionation of the treatment scheme. The crucial role of the product of the radiosensitivity coefficient α and the tumour cell doubling time T_P on the optimal duration of the whole treatment has been highlighted.

Key words: Nonlinear programming, cancer radiotherapy, linear-quadratic model

AMS subject classifications: 90C30, 90C90, 92B05

1. Introduction

Many different approaches have been proposed to improve the outcome of cancer radiotherapy treatments, including the development of accurate diagnostic techniques, treatment planning and clinical dosimetry, as well as novel modalities of radiation delivery. All the methods, both experimental and theoretical, share the goal of achieving the best compromise between the efficacy and the safety of the treatment by means of the maximization of the tumour damage along with the minimization/limitation of the toxicity to the surrounding normal tissues. The proposed approaches are mainly based on optimization methods of the irradiation protocol and on techniques of spatial optimization of the dose distribution. The protocol optimization methods search for the optimal size and number of dose fractions, as well as for the optimal overall treatment time. Conversely, the spatial optimization techniques explicitly account for the geometry of the tumour and of the surrounding normal tissues to provide the optimal volume distribution of the radiation dose intensity (see for instance the book by Li et al. (2012)).

As far as the protocol optimization methods are concerned, a wide variety of different empirical, analytical and numerical approaches have been proposed in the last three decades, usually based on mathematical models of the radiation response of tumour and normal cells. The model most regularly used to represent the relation between a single radiation dose d (Gy) and the fraction S of cells surviving the irradiation is the linear-quadratic (LQ) model (Thames, 1985; Fowler, 1989; Jones and Dale, 1999)

$$S = \exp(-\alpha d - \beta d^2)\,, \tag{1}$$

where α and β are the radiosensitivity parameters. In (1), the linear term accounts for non repairable lesions to the DNA, while the quadratic term accounts for lethal misrepair events following DNA double strand breaks (Hlatky et al., 1994).

The reason of the wide acceptance of the LQ model, and of its extensive use in radiotherapy, lies in the combination of the simple formalism derived from biophysical principles, with the flexibility of the model in representing the radiation response of different kinds of tissues, either healthy and tumoural, in the clinically meaningful dose range (Brenner, 2008; Kirkpatrick et al., 2008).

Although the radiation response is dominated by the instantaneous cell killing following a single irradiation (given by the argument of the exponential in Eq. (1)), other fractionation/protraction effects underlying the cell response have to be taken into account when multiple sessions are delivered. The LQ model has also been largely exploited in its extended LQR version proposed by Brenner et al. (1995), that includes other processes characterizing the cell response to multiple irradiations. Such processes are the repair of the radiation damage, the resensitization mechanisms, i.e. the redistribution of cells among the cell-cycle phases and the reoxygenation of tissues, and the repopulation due to the regrowth of cells surviving irradiation (Wong and Hill, 1998). Concerning the cell redistribution within the replicative cycle, simulation models with cell-cycle structure have been proposed to account for the different phase-specific radiosensitivities of cells (Dionysiou et al., 2004; Ribba et al., 2006). The kinetic effects of repopulation and reoxygenation have been modeled in studies where the geometry of the tumour mass was explicitly taken into account (Düchting et al., 1992, 1995; Bertuzzi et al., 2008, 2010). A very recent study has been proposed by Harriss-Philips et al. (2016) to predict cell kill during radiotherapy, taking into account the effects of tumour hypoxia and reoxygenation. Comparisons of different (high-dose versus conventional) radiotherapy schemes are provided, incorporating probabilistic parameter distributions and using both linear-quadratic and linear-quadratic-cubic models.

While the resensitization process, as well as the sublethal damage due to incomplete repair among fractions, have been shown to scarcely affect the optimal treatment schedules, the repopulation effect is a crucial factor in evaluating the efficacy of radiation treatments (Yang and Xing, 2005; Bertuzzi et al., 2013). A recent review by O'Rourke et al. (2009) examines the LQ formalism with emphasis on the modelling of redistribution mechanisms and repopulation laws, such as exponential, Gompertzian and logistic laws.

On the basis of the LQ and the LQR models, different approaches looking to the optimization of the radiotherapeutic strategy have been proposed. For instance, Fowler (2007, 2008) used the LQ model with the repopulation term to investigate optimal schedules for head and neck cancer, taking into account both the early reacting normal tissues and the late complications. The author proposed an empirical procedure to optimize the total duration of the treatment, keeping the late tissue damage fixed and using uniform fractionation schedules. The importance of the radiosensitivity ratio α/β in determining the optimal fractionation strategy is pointed out and relationships between kick-off time and optimal treatment length are evidenced. The findings about the optimal treatment time agree with the results reported by Yang and Xing (2005), who investigated optimal radiotherapy schemes for fast proliferating and slowly proliferating tumours by means of a simulated annealing procedure, using the complete LQR model with parameter values taken from the literature. The optimization procedure searches for the highest tumour biologically effective dose (BED) over the total treatment length (with constant late normal tissue BED) and optimal fractionation scheme not necessarily uniform are obtained. In particular, while equi-fractionated schemes proved to be optimal for fast proliferating tumours, hypofractionated schedules are required for slowly proliferating tumours. This numerical result has been confirmed by Mizuta et al. (2012) who used the LQ model, not including the repopulation term, to represent the response of tumours and a single normal tissue. In particular, the expression of the optimal dose fraction size was analytically derived for tumours characterized by a radiosensitivity ratio higher or lower than the radiosensitivity ratio of the considered normal tissue. Bortfeld et al. (2015) exploited the results by Mizuta et al. (2012) to explicitly study the effect of tumour repopulation on the optimal dose delivery, by considering different tumour growth models (exponential vs Gompertzian growth) and a single organ at risk constraint. In case of Gompertzian growth, the optimal fractionation schemes are found to consist of larger fraction sizes towards the end of the treatment.

The analytical expression of the optimal solution was obtained also by Bertuzzi et al. (2013), who considered an optimal radiotherapy problem, describing the tumour and normal tissue responses by the LQ model including the repopulation term and the sublethal damage term due to incomplete repair. Assuming that the number of treatment weeks was fixed and that it was assigned some rule to distribute over the weeks the total tolerable damage to healthy tissues, the optimization problem was formulated with respect to the fraction sizes of a single week (one fraction/day, five fractions/week). A similar radiotherapy optimization problem over a fixed treatment length was considered by Bruni et al. (2015), where a new constraint consisting of an upper bound for the daily fraction was introduced in order to strengthen the normal tissue constraints, especially with respect to late complications possibly occurring months or years after irradiation.

In the recent study by Badri et al. (2016) heuristic optimization techniques are used to find radiation delivery schedules providing survival benefit over standard fractionation schedules. The study combines the LQ framework with a dynamic model of glioblastoma, a fast proliferating brain tumour, accounting for two separate populations of cells: stem-like radio-resistant glioma

cells and differentiated radiosensitive glioma cells. Two kind of normal tissues are considered (early-responding tissue, such as skin, and slow-responding tissue, such as neurons) and two constraints are imposed to guarantee that the radiation damage to normal tissue does not exceed prescribed levels. The optimal total dose, number of fractions, dose per fraction and inter-fraction intervals are identified considering schedules constrained to have a fixed treatment duration and lower limits on the fraction sizes and inter-fraction intervals.

Saberian et al. (2015) presented the mathematical formulation of an optimal fractionation problem based on the LQ model that includes exponential tumour regrowth after a time-lag. The model takes into account sparing factors resulting from a spatially optimized fluence-map which is the input for the protocol optimization problem. The formulation incorporates maximum dose, mean dose and dose-volume constraints on multiple normal tissues leading to a mixed-integer, non-convex quadratic programming problem with multiple quadratic constraints. Based on the prevalent estimates of tumour and normal tissue parameters, the authors simplify the problem by establishing sufficient conditions for the optimality of a single dose fraction or of an equi-fractionated protocol. Numerical simulation of tumour test cases satisfying the conditions previously established are performed to find the optimal number of fractions.

It is worth mentioning studies related to optimization techniques in radiotherapy, where the geometry of tumour and organs at risk are explicitly taken into account to perform the spatial optimization of the dose distribution, namely the studies focusing on intensity-modulated radiation therapy (IMRT). For instance, the LQR model has been used by Lee et al. Lee et al. (2006) in a mixed integer programming procedure for improving the 3-D distribution of the radiation dose by determining the optimal beam angles and intensities in IMRT. Optimal adaptive fractionation schemes accounting for variations of the relative positions between tumour and healthy tissues during the treatment have been derived by Lu et al. (2008a,b). A further application of cancer treatment optimization has been presented by Ledzewicz and Schättler (2012), where a model of the tumour dynamics under radio and anti-angiogenic therapy is analyzed, and an optimal control problem is set up with the objective of minimizing the tumour volume subject to constraints limiting the negative effects on healthy tissues.

In the context of external beam radiotherapy (EBRT), the present work aims to find the optimal sheme of dose fractionation, in terms of daily size and number of fractions, as well as the optimal treatment duration of radiotherapy protocols of the kind one fraction/day, five fractions/week with weekend breaks. It originates from the paper by Bruni et al. (2015), extending the analytical study of the protocol optimization over a single week of treatment proposed in that paper. In particular, we provide i) the analytical solution for the optimization problem of the dose fractionation over a fixed but arbitrary treatment duration, ii) the numerical search of the optimal number of fractions and therefore of the optimal treatment time. This partly analytical and partly numerical approach is similar to that followed by Saberian et al. (2015) and Badri et al. (2016), although some differences are present in the problem formulation. In particular, the protocol optimization problem is formulated considering constraints on the maximal tolerable damage to two kind of normal tissues (early and late responding), and including an additional constraint on the maximal value of the daily fraction size (Section 2). We represented the tumour and healthy tissue responses to radiation by means of the LQ model assuming that accelerated exponential repopulation occurs after a time-lag, thus disregarding kinetic effects related to fractionation/protraction of the dose as well as any possible spatial heterogeneity in the cell response. Exponential regrowth is also taken into account for early reacting normal tissues. By means of this formulation, and in view of the type of protocols considered, in Section 3 we provide a frame-

work for determining analytically the optimal fractionation of the radiation dose as a function of tumour type. In particular, the optimal protocol structure is completely identified by the tumour radiosensitivity ratio, while the sizes of the daily doses only depend on the normal tissue parameters and on the daily fraction upper bound. Finally, the numerical simulations presented in Section 4 focus on three tumour classes characterized by different radiosensitivity ratios. For all the classes considered, we set nominal normal tissue parameters, according to indications derived from the literature (Thames et al., 1990; Yang and Xing, 2005; Fowler, 2010), and we investigate how the optimal solution is affected by changes of both the tumour parameters and the upper bound on the daily dose.

A remarkable result emerging from the present study is that the tumour α/β ratio affects the fractionation scheme, in that the conventional uniform fractionation is optimal for tumours having large radiosensitivity ratio while hypofractionation is convenient for small α/β ratios. It is shown in the following how the extent of tumour repopulation influences the optimal treatment length.

2. Formulation of an optimal constrained radiotherapy problem

The aim of this work is to determine optimal fractionated protocols in EBRT, typically administered during weekdays with weekend breaks. We formulate a general problem of radiotherapy optimization, which consists in determining the therapeutic protocol that maximizes the tumour damage while keeping the damages to normal tissues below assigned tolerable levels. We consider two kind of normal tissues that is early and late responding tissues, typically associated to α/β ratios of 10 Gy and 3 Gy respectively (Thames et al., 1990; Fowler et al., 2003a; Yang and Xing, 2005). In principle, such an optimization problem should be formulated with respect to three decision variables: size and number of dose fractions, and total treatment time. However, we consider protocols of the kind one fraction/day, five fractions/week, so that we can assume the following relationship between the overall treatment time, $T(n)$ (days), and the maximal number n of dose fractions deliverable over this time:

$$T(n) = 7\left[\frac{n}{5}\right] - 1 - \begin{cases} 2, & \text{n/5 integer,} \\ 5\left[\frac{n}{5}\right] - n, & \text{else.} \end{cases} \tag{2}$$

Such a fixed relationship allows to consider as the only decision variables of the optimization problem the number and the sizes of the dose fractions. Obviously, expressions of $T(n)$ different from (2) could be envisaged in the problem formulation to represent different schemes of radiotherapy administration, such as for instance two fractions/day or without weekend interruptions, without substantially altering the solving procedure.

The problem formulation is based on the LQ model of the tumour and normal tissue survival including tumour regrowth after a constant lag time, with a constant exponential rate over the treatment length. The choice on the growth law might be questionable as saturating growth laws, like the logistic or the Gompertzian laws, could appear more appropriate. However, O'Rourke et al. (2009) found that tumours following exponential or logistic repopulation mechanisms resulted in similar survival outcomes, although generally higher than those obtained assuming a Gompertzian nature of repopulation. Moreover, it is widely accepted that exponential growth can adequately represent the tumour kinetics over limited time lengths, such as the typical radiation treatment lengths. For the sake of simplicity, we do not consider the redistribution and

reoxygenation effects, since they scarcely affect the optimal treatment schedules (Yang and Xing, 2005; Bertuzzi et al., 2013).

Let us consider a homogeneous cell population subject to a radiation treatment consisting of n not necessarily equal dose fraction d_k, $k = 1, \dots, n$, administered over a total time $T(n)$. According to the LQ model, the logarithmic fraction of cells surviving the treatment is given by

$$\ln(S) = -\alpha \sum_{k=1}^{n} d_k - \beta \sum_{k=1}^{n} d_k^2 + \frac{\ln(2)}{T_P}\big(T(n) - T_K\big) H\big(T(n) - T_K\big)\,, \tag{3}$$

where α and β are the radiosensitivity parameters accounting for non-repairable lesions to DNA and, respectively, for the lethal misrepair events occurring in the repair process of DNA double strand breaks, T_P is the repopulation doubling time, T_K is the kick-off time at which compensatory proliferation starts, and $H(\cdot)$ is the unitary step Heaviside function accounting for the onset of repopulation after T_K. The overall radiation damage M is defined as $M = -\ln(S)$.

Representing by the LQ model the response to radiation of both tumour and surrounding normal tissues, the problem is that of minimizing the logarithmic tumour survival (3) with respect to the dose fraction sizes d_k, $k = 1, \dots, n$, as well as to their number n, under the constraint of keeping the damages to the early and late responding normal tissues below maximal admissible levels $M_e, M_l > 0$:

$$\alpha_e \sum_{k=1}^{n} d_k + \beta_e \sum_{k=1}^{n} d_k^2 - \frac{\ln(2)}{T_{Pe}}\big(T(n) - T_{Ke}\big) H\big(T(n) - T_{Ke}\big) \le M_e\,, \tag{4}$$

$$\alpha_l \sum_{k=1}^{n} d_k + \beta_l \sum_{k=1}^{n} d_k^2 \le M_l\,, \tag{5}$$

where the parameters have been indexed by subscripts "e" and "l" when referring to the early and late tissues respectively. The cell repopulation term is absent in constraint (5) as it is negligible for late responding tissues (Fowler, 2012).

While the LQ model is widely accepted to describe the acute cell reaction induced by the exposure to radiation, the prediction of late complications by means of the same model is controversial, especially for high fraction doses (Yang and Xing, 2005; Astrahan, 2008; Brenner, 2008; Kirkpatrick et al., 2008, 2009; Macchia et al., 2010; Ling et al., 2010). For this reason, in addition to the constraints (4) and (5) we introduce a constraint directly limiting the daily radiation dose and we set, as done in the paper by Bruni et al. (2015), an upper bound d_M on the dose fraction size.

Let us introduce the notation

$$\rho = \frac{\alpha}{\beta}, \quad \rho_e = \frac{\alpha_e}{\beta_e}, \quad \rho_l = \frac{\alpha_l}{\beta_l}, \tag{6}$$

$$k_e(n) = \frac{1}{\beta_e}\left[M_e + \frac{\ln(2)}{T_{Pe}}\big(T(n) - T_{Ke}\big) H\big(T(n) - T_{Ke}\big)\right], \tag{7}$$

$$k_l = \frac{M_l}{\beta_l}, \tag{8}$$

with $\rho_e > \rho_l$ (Fowler, 2012).

We can set the following optimization problem, in terms of the variables n (number of fractions) and d, the vector of the dose fractions d_k, $k = 1, \dots, n$.

Problem 2.1. *Minimize the function:*

$$J(n,d) = -\rho \sum_{k=1}^{n} d_k - \sum_{k=1}^{n} d_k^2 + \frac{\ln(2)}{\beta T_P}\big(T(n) - T_K\big) H\big(T(n) - T_K\big)\,, \tag{9}$$

on the admissible domain :

$$D = N \times D_n \tag{10}$$

where

$$N = \{n \in \mathbb{N} | 1 \le n \le n_M\}\,, \tag{11}$$

$$\begin{aligned} D_n = \{d \in \mathbb{R}^n \;\; | \;\; & g_e(n,d) = \rho_e \sum_{k=1}^{n} d_k + \sum_{k=1}^{n} d_k^2 - k_e(n) \le 0\,, \\ & g_l(n,d) = \rho_l \sum_{k=1}^{n} d_k + \sum_{k=1}^{n} d_k^2 - k_l \le 0\,, \\ & 0 \le d_k \le d_M\,,\; k = 1, \ldots, n\}\,. \end{aligned} \tag{12}$$

We decompose Problem 2.1 into a finite collection of n_M optimization subproblems to be solved in cascade with respect to $d \in D_n$ for n fixed, and then with respect to n, for any $n \in N$. Recalling the espressions (10)–(12) of the feasible set D, we can write

$$\min_{(n,d)\in D} J(n,d) = \min_{n \in N} \left(\min_{d \in D_n} J(n,d) \right)\,. \tag{13}$$

The cost function $J(n,d)$ can be written as the sum

$$J(n,d) = J_n(d) + E(n)\,, \tag{14}$$

with

$$J_n(d) = -\rho \sum_{k=1}^{n} d_k - \sum_{k=1}^{n} d_k^2\,, \tag{15}$$

and

$$E(n) = \frac{\ln(2)}{\beta T_P}\big(T(n) - T_K\big) H\big(T(n) - T_K\big)\,. \tag{16}$$

Observing that $E(n)$ in (16) does not depend on the doses, the problem of minimizing $J(n,d)$ on D_n is equivalent to that of minimizing $J_n(d)$ on the same set. So, we consider the following optimization problem.

Problem 2.2. *For any fixed $n \in N$, minimize the function $J_n(d)$ in* (15) *with respect to d on the admissible set D_n in* (12)*.*

The decomposition (13) evidences that the Problem 2.1 admits an optimal solution. Indeed, the compactness of D_n and the continuity of $J_n(d)$ on D_n guarantee, according to the Weierstrass Theorem, the existence of an optimal solution for Problem 2.2 for any given $n \in N$. Let us denote by $d_n^\star$ such an optimal solution, defining

$$J^\star(n) \triangleq J(n, d_n^\star) = \min_{d \in D_n} J(n,d)\,. \tag{17}$$

Next, being N of finite cardinality equal to n_M, it is possible to determine the optimum of Problem 2.1 by means of a finite number of direct comparisons among the values of $J^\star(n)$ for $n \in N$. In Section 4, we seek the optimum over N by means of numerical simulations, under different parameter settings taken from the literature.

However, finding the optimal solutions of Problem 2.1 through the decomposition (13), namely by optimizing firstly with respect to the dose sizes, and then with respect to the dose number, means to take separately into account the contributions to the cell response owed to the radiation LQ damage and to the compensatory repopulation. We remark that with n set to a fixed integer, the overall treatment time $T(n)$, and consequently $k_e(n)$, are constant in Problem 2.2. Therefore, all the radiation treatments which are candidates to the optimum of Problem 2.2 have the same duration $T(n)$. In other words, $T(n)$ represents the time after which the damages produced by all protocols of length n are evaluated, even though, as a consequence of the constraints $d_k \geq 0$, some dose fractions can be zero.

3. Optimal solutions for a fixed n

The optimal solutions of Problem 2.2 can be derived by extending to a generic dose number $n \in [1, n_M]$ the results demonstrated by Bruni et al. (2015) for the problem formulated over a week of treatment, that is with $n = 5$. In fact, we obtained the optimal solutions of that problem by solving the system of necessary and admissibility conditions provided by the Karush-Kuhn-Tucker Theorem (KKT). Because of the particular problem structure, where either the cost function and the constraints are symmetrical with respect to the n-dimensional line

$$\ell = \{d \in \mathbb{R}^n : d_i = d_{i+1}, i = 1, \ldots, n-1\}, \tag{18}$$

when n increases, the necessary and admissibility conditions increase in number while their structure remains unchanged. In Appendix A, we report the complete set of Karush-Kuhn-Tucker conditions for Problem 2.2 with a generic n, whereas in the present section we give some results and properties relevant to the optimal solutions of Problem 2.2, omitting the proofs when they are straightforward extensions of the results proved in the paper by Bruni et al. (2015).

The first property concerns the admissible domain of Problem 2.2 and precisely the region defined by the early and late normal tissue constraints. The inequalities $g_e(n, d) \leq 0$, $g_l(n, d) \leq 0$ represent two hyperspheres of $\mathbb{R}^n$ that have centers on the negative half of the line ℓ and that certainly contain points of the positive orthant of $\mathbb{R}^n$ including the axis origin, since $k_e(n) > 0$, $k_l > 0$. The insersection region between these positive parts of the hyperspheres, may coincide with the region identified in the positive orthant of $\mathbb{R}^n$ by just one of the normal tissue constraints, which is then prevalent. We remind that the geometric prevalence of one constraint means that points satisfying the prevalent constraint make the other strictly satisfied, so that the latter constraint becomes unnecessary. The geometry of the early and late constraints, and in particular whether there is a prevalent contraint or not, depends on the sign of the differences $k_e(n) - k_l$, $\rho_e k_l - \rho_l k_e(n)$, and on the global parameter v defined as

$$v \triangleq \frac{(k_e(n) - k_l)^2}{(\rho_e - \rho_l)(\rho_e k_l - \rho_l k_e(n))}. \tag{19}$$

For a generic fixed n, the relation between normal tissue parameters and geometry of the corresponding constraints is illustrated in Table 1, with $k_e(n)$ and k_l computed according to (7),(8) and $\rho_e > \rho_l > 0$.

Table 1: Relationship between normal tissue parameters and geometry of the admissible domain.

Geometry	Model parameters
Prevalent early constraint	$k_e(n) - k_l \leq 0$
	$k_e(n) - k_l > 0,\ \rho_e k_l - \rho_l k_e(n) > 0,\ v < 1$
No prevalent constraint	$k_e(n) - k_l > 0,\ \rho_e k_l - \rho_l k_e(n) > 0,\ 1 \leq v \leq n$
Prevalent late constraint	$k_e(n) - k_l > 0,\ \rho_e k_l - \rho_l k_e(n) > 0,\ v > n$
	$k_e(n) - k_l > 0,\ \rho_e k_l - \rho_l k_e(n) \leq 0$

We note that the constraints $d_i \leq d_M$, $i = 1, \ldots, n$, have no influence on the geometric situations depicted in Table 1, since the dose upper bound has the effect of clipping out of the feasible region portions of the early and late hyperspheres with points exceeding the dose limit, without modifying their relative position.

In order to examine the interaction between the upper limit d_M and the normal tissue constraints, we introduce the set

$$B_n = \{d \in \mathbb{R}^n : 0 \leq d_k \leq d_M, k = 1, \ldots, n\}, \tag{20}$$

and the disjoint sets

$$\begin{aligned} H_1 &= B_n \cap \{d \in \mathbb{R}^n : g_e(n,d) = 0,\ g_l(n,d) = 0\}, \\ H_2 &= B_n \cap \{d \in \mathbb{R}^n : g_e(n,d) < 0,\ g_l(n,d) = 0\}, \\ H_3 &= B_n \cap \{d \in \mathbb{R}^n : g_e(n,d) = 0,\ g_l(n,d) < 0\}, \\ H_4 &= B_n \cap \{d \in \mathbb{R}^n : g_e(n,d) < 0,\ g_l(n,d) < 0\}, \end{aligned} \tag{21}$$

such that $D_n = H_1 \cup H_2 \cup H_3 \cup H_4$. We deal with the more general case in which there is not a prevalent normal tissue constraint and the optimal solution may in principle belong to any of the sets (21). When, on the contrary, one of the normal tissue constraints is more restrictive than the other for any $d \in D_n$, some set in (21) is empty irrespective of d_M: certainly, it is $H_1 = \emptyset$, while it is $H_2 = \emptyset$ for prevalent early constraint and $H_3 = \emptyset$ for prevalent late constraint.

We report some extensions of the results of Bruni et al. (2015) (Theorem 1, Corollaries 1-4).

Property 1 If the dose upper bound is such that

$$d_M \geq \min\{A_e(n,0), A_l(n,0)\}, \tag{22}$$

where

$$A_e(n,0) = -\frac{\rho_e}{2} + \sqrt{\left(\frac{\rho_e}{2}\right)^2 + \frac{k_e(n)}{n}}, \qquad A_l(n,0) = -\frac{\rho_l}{2} + \sqrt{\left(\frac{\rho_l}{2}\right)^2 + \frac{k_l}{n}}, \tag{23}$$

the optimal solution must satisfy at least one of the equality constraints $g_e(n,d) = 0$ or $g_l(n,d) = 0$, so as to produce the maximal admissible damage to one or both the normal tissues. Therefore the optimum must belong to one of the sets H_i, $i = 1, 2, 3$.

On the contrary, if

$$d_M < \min\{A_e(n,0), A_l(n,0)\}, \tag{24}$$

it is $H_i = \emptyset$, for $i = 1, 2, 3$, $D_n \equiv H_4 \equiv B_n$, and the only optimal solution is the vector $d_n^\star = \tilde{d}$, with $d_k = d_M, k = 1, \ldots, n$. ∎

According to this result, the optimal solution of Problem 2.2 is completely specified when d_M satisfies the condition (24). Let us add some comments about the sets H_1, H_2, H_3 under the opposite and more meaningful condition (22) for d_M.

All the points belonging to H_1 have sum of the doses and sum of the squared doses independent of the point itself and given by

$$\sum_{k=1}^{n} d_k = \frac{k_e(n) - k_l}{\rho_e - \rho_l} \triangleq S\,, \tag{25}$$

$$\sum_{k=1}^{n} d_k^2 = \frac{\rho_e k_l - \rho_l k_e(n)}{\rho_e - \rho_l} \triangleq Q\,. \tag{26}$$

This property is immediately deduced from the equations of the normal tissue constraints that define H_1, upon representing the sum of the doses and the sum of the squared doses in explicit form. Similarly, it can be seen that points of H_2 satisfy $g_l(n, d) = 0$ and the inequalities

$$\sum_{k=1}^{n} d_k < S\,, \qquad \sum_{k=1}^{n} d_k^2 > Q\,, \tag{27}$$

while points of H_3 are such that $g_e(n, d) = 0$ and

$$\sum_{k=1}^{n} d_k > S\,, \qquad \sum_{k=1}^{n} d_k^2 < Q\,. \tag{28}$$

We observe that the definitions (25) and (26) lead to the further interpretation of the quantity v in (19) as

$$v = \frac{S^2}{Q}\,. \tag{29}$$

Two further properties relevant to the solution structure under (22) can be deduced developing the necessary and admissibility conditions for Problem 2.2.

Property 2 The system of necessary and admissibility conditions admits a finite number of isolated solution points in $H_1 \cup H_2 \cup H_3$. Solution points of this kind contain at most three values: the limit values 0 and d_M, and an intermediate value that can be univocally determined by solving the equation related to the normal tissue constraint being active. Thus, such solutions are completely characterized by their "structure", i.e. by the number of dose fractions equal to the three values mentioned above. We denote by $d_e(i, j)$ and $d_l(i, j)$ the structured solutions satisfying the equalities $g_e(n, d) = 0$, and respectively $g_l(n, d) = 0$, that have j entries equal to the upper bound d_M, i entries equal to the intermediate value and, consequently, $n - i - j$ zero entries. The intermediate values in the vectors $d_e(i, j)$ and $d_l(i, j)$ are given by

$$A_e(i, j) = -\frac{\rho_e}{2} + \sqrt{\left(\frac{\rho_e}{2}\right)^2 + \frac{k_e(n) - j d_M(d_M + \rho_e)}{i}}\,, \tag{30}$$

and

$$A_l(i,j) = -\frac{\rho_l}{2} + \sqrt{\left(\frac{\rho_l}{2}\right)^2 + \frac{k_l - j d_M(d_M+\rho_l)}{i}}\,. \tag{31}$$

It is evident from the formulation of Problem 2.2 that vectors $d_e(i,j)$, $d_l(i,j)$ having the same pair of indexes i, j are indistinguishable, that is equivalent with respect to the cost function. Therefore, for a fixed i, j, the notation $d_e(i,j)$, $d_l(i,j)$ refers to a whole class of equivalent structures.

In addition to the mentioned solutions, if $\rho_l \le \rho \le \rho_e$, the KKT system has an infinite set of solutions without a particular structure and all cost-equivalent. Such a solution set coincides with the set H_1 for $\rho_l < \rho < \rho_e$, with $H_1 \cup H_2$ for $\rho = \rho_l$, and with $H_1 \cup H_3$ for $\rho = \rho_e$. ∎

Property 3 Given a pair i, j, only one of the vectors $d_e(i,j)$, $d_l(i,j)$ is admissible (unless $A_e(i,j)$ and $A_l(i,j)$ coincide) and in particular the vector containing the smallest intermediate dose. Such a property is easily verified noting that $d_e(i,j)$ is a feasible vector if and only if $g_l(n, d_e(i,j)) \le 0$, which amounts to say $A_e(i,j) \le A_l(i,j)$ and, similarly, $d_l(i,j)$ is admissible if and only if $g_e(n, d_l(i,j)) \le 0$, which amounts to say $A_l(i,j) \le A_e(i,j)$.

For $j = 0$, as there are no d_M values in the vectors, it is easy to establish which vector of the pair $d_e(i,0)$, $d_l(i,0)$ is admissible. To this end, we rewrite $g_e(n,\cdot)$ and $g_l(n,\cdot)$ as functions of a generic variable x, for a given $1 \le i \le n$,

$$y_e = ix^2 + i\rho_e x - k_e(n)\,, \qquad y_l = ix^2 + i\rho_l x - k_l\,, \tag{32}$$

and we compare the positive zeroes of y_e, y_l which are respectively given by

$$A_e(i,0) = -\frac{\rho_e}{2} + \sqrt{\left(\frac{\rho_e}{2}\right)^2 + \frac{k_e(n)}{i}}\,, \quad A_l(i,0) = -\frac{\rho_l}{2} + \sqrt{\left(\frac{\rho_l}{2}\right)^2 + \frac{k_l}{i}}\,. \tag{33}$$

The functions (32) have the unique intersection point

$$x_i = \frac{k_e - k_l}{i(\rho_e - \rho_l)} > 0\,, \qquad y_i = \frac{1}{i}\left(\frac{k_e - k_l}{\rho_e - \rho_l}\right)^2 + \frac{\rho_l k_e - \rho_e k_l}{\rho_e - \rho_l}\,,$$

so that the ordering of $A_e(i,0)$ and $A_l(i,0)$ depends only on the sign of y_i. It can be noticed that setting $i = v$, where v is defined in (19), the intersection ordinate becomes equal to zero and the two roots coincide. So, if $i < v$, we have $y_i > 0$ and it is $A_l(i,0) < A_e(i,0)$, whereas if $i > v$, it is $y_i < 0$ and $A_e(i,0) < A_l(i,0)$. In short, we have

$$\min\{A_e(i,0), A_l(i,0)\} = \begin{cases} A_l(i,0)\,,\ i = 1 \,\ldots\, [v]\,, \\ A_e(i,0)\,,\ i = \min\{[v]+1,\, n\}, \ldots, n\,. \end{cases} \tag{34}$$

∎

The expressions (33) show that $A_e(i,0)$ and $A_l(i,0)$ decrease as i increases which, along with the partition (34), imply the following ordering among the n minima in (34):

$$A_e(n,0) < \ldots < A_e([v]+1,0) < A_l([v],0) < \ldots < A_l(1,0)\,, \tag{35}$$

where $[v] \le n-1$ has been implicitly assumed, or in (35) only "late" solutions $A_l(i,0)$, $i = 1, \ldots n$, are present.

Some results suitable to determine which values of d_M allow set (21) to contain the optimal solution in the absence of a prevalent constraint are given below.

Lemma 3.1. *For $k_e(n) - k_l > 0$, $\rho_e k_l - \rho_l k_e(n) > 0$, and $1 \leq v \leq n$ the following conditions about the non-emptiness of the sets* (21) *hold:*

i) $H_1 \neq \emptyset$ if and only if $d_M \geq R_{1[v]}$,

ii) $H_2 \neq \emptyset$ if and only if $d_M > R_{1[v]}$ and $v \neq 1$,

iii) $H_3 \neq \emptyset$ if and only if $d_M \geq A_e(n,0)$ and $v \neq n$,

iv) $H_4 \neq \emptyset$ for any d_M,

where

$$R_{1[v]} = \frac{S}{[v]+1}\left(1 + \sqrt{\frac{[v]+1-v}{v[v]}}\right), \tag{36}$$

with v defined by (19) *and S by* (25)*, and $A_e(n,0)$ given by* (23)*.*

Proof. The implication $\{H_1 \neq \emptyset \Rightarrow d_M \geq R_{1[v]}\}$ of point i) can be proved by contradiction showing that if $d_M < R_{1[v]}$, H_1 must be empty. Because of the symmetry of H_1 with respect to the line (18), we decompose H_1 into the union of $n!$ subsets, each obtained selecting a possible ordering among the n doses d_k. Thus, without loss of generality, we consider the subset

$$\tilde{\Omega}_1 = \{d \in \mathbb{R}^n : g_e(n,d) = 0,\, g_l(n,d) = 0\,,\, d_M \geq d_n \geq d_{n-1} \geq \ldots \geq d_1 \geq 0\}\,, \tag{37}$$

and we prove that $d_M < R_{1[v]}$ implies $\tilde{\Omega}_1 = \emptyset$. Since the same implication is true for any subset of the kind (37), proving the property in $\tilde{\Omega}_1$ is sufficient to prove it in the whole H_1. Let us write $\tilde{\Omega}_1 = B_n \cap \Omega_1$, with

$$\Omega_1 = \{d \in \mathbb{R}^n : g_e(n,d) = 0,\, g_l(n,d) = 0\,,\, d_n \geq d_{n-1} \geq \ldots \geq d_1 \geq 0\}\,. \tag{38}$$

The validity of the property in $\tilde{\Omega}_1$ can be seen by proving that

$$\min_{d \in \Omega_1} d_n = R_{1[v]}\,. \tag{39}$$

An outline of the procedure to solve the optimization problem (39) is given in Appendix B. More details can be found in the report by Conte et al. (2015) where it is also shown that the unique minimum point is the vector d^R composed by $[v]$ components equal to $R_{1[v]}$, one component equal to $S - [v]R_{1[v]}$ (this entry is absent for $v = n$), plus $n - [v] - 1$ components equal to zero (absent if $v \geq n-1$). Therefore, if $d_M < R_{1[v]}$ the set $\tilde{\Omega}_1$ (as well as any other set obtained taking a different dose ordering) is empty. Hence, H_1 is empty.

We notice that the vector d^R satisfies by construction both the early and late constraints with the equality sign. This property also constitutes a direct proof of the implication $\{d_M \geq R_{1[v]} \Rightarrow H_1 \neq \emptyset\}$ of point i), in that for any $d_M \geq R_{1[v]}$ we have $d^R \in B_n$ and then $d^R \in H_1$.

Moreover, let us underline that, according to Conte et al. (2015), $R_{1[v]}$ is such that

$$A_e([v]+1,0) < R_{1[v]} \leq A_l([v],0)\,, \tag{40}$$

with the equality sign holding if and only if v is an integer number, i.e. $v = [v]$. Then, it is

$$R_{1[v]} = A_l([v], 0) = A_e([v], 0) = \frac{S}{[v]}\,, \tag{41}$$

the intermediate dose of the vector d^R, $S - [v]R_{1[v]}$, vanishes (or is absent for $v = n$), and we have $d^R = d_e([v], 0) = d_l([v], 0)$.

Concerning the proof of point ii), we start by showing that for $v = 1$, the set H_2 is empty. Recalling (29), $v = 1$ means $S^2 = Q$. Since the dose fractions d_k are non negative quantities, and being the constraints (27) valid in H_2, points of H_2 are such that

$$S^2 > \left(\sum_{k=1}^{n} d_k\right)^2 > \sum_{k=1}^{n} d_k^2 > Q\,,$$

which is conflicting with the condition $v = 1$.

Let us now prove that $d_M \leq R_{1[v]}$ implies $H_2 = \emptyset$. Proceeding similarly to the previous point i), we can prove (see Appendix B and Conte et al. (2015)) that the minimization problem

$$\min_{d \in \Omega_1 \cup \Omega_2} d_n\,, \tag{42}$$

with Ω_1 in (38) and

$$\Omega_2 = \{d \in \mathbb{R}^n : g_e(n, d) < 0,\, g_l(n, d) = 0\,,\, d_n \geq d_{n-1} \geq \ldots \geq d_1 \geq 0\}\,, \tag{43}$$

again admits the unique optimal solution $R_{1[v]}$ attained at the point d^R, which belongs to Ω_1 as seen above. Denoting by $\tilde{\Omega}_2 = \Omega_2 \cap B_n$, this result is sufficient to state that $d_M \leq R_{1[v]}$ implies $\tilde{\Omega}_2 = \emptyset$. So, if $d_M < R_{1[v]}$, both the sets $\tilde{\Omega}_1$ and $\tilde{\Omega}_2$ are empty, while if $d_M = R_{1[v]}$, it is $\tilde{\Omega}_1 \cup \tilde{\Omega}_2 \equiv \{d^R\}$, so that $\tilde{\Omega}_2$ is empty. Then, for $d_M \leq R_{1[v]}$ the set H_2 is empty.

The non-emptiness of H_2 for $d_M > R_{1[v]}$ and $v \neq 1$ can be proved showing the existence of at least one vector that belongs to H_2 when d_M exceeds $R_{1[v]}$. Since for $d_M = R_{1[v]}$, the vector $d^R \in H_1$ actually equals the structure $d_l(1, [v]) = d_e(1, [v])$, we construct the sought vector of H_2 starting from this structure, letting d_M increase above $R_{1[v]}$ and moving along $g_l(n, d) = 0$ or $g_e(n, d) = 0$. It is necessary to distinguish between $v \neq [v]$ and $v = [v]$ because d^R has $[v] + 1$ non zero entries for $v \neq [v]$, and $[v]$ non zero entries for v integer. Also, it is useful to recall that $A_l(i, 0) \leq A_e(i, 0)$, for $i \leq [v]$ in view of (34).

For $v \neq [v]$, set $d_M = R_{1[v]} + \zeta$, with $0 < \zeta \leq A_l([v], 0) - R_{1[v]}$, and consider the vectors $d_l(1, [v])$, $d_e(1, [v])$ having $[v]$ entries equal to d_M and the intermediate entries $A_l(1, [v])$, $A_e(1, [v])$ respectively given by (31), (30). We intend to show that $A_l(1, [v]) < A_e(1, [v])$ for $\zeta \in (0, A_l([v], 0) - R_{1[v]}]$, so that $d_l(1, [v])$ is the requested vector of H_2. Indeed, $A_l(1, [v])$, $A_e(1, [v])$ are decreasing functions of ζ in the mentioned interval and for $\zeta \to 0^+$, both $A_l(1, [v])$ and $A_e(1, [v])$ tend to $S - [v]R_{1[v]}$. Moreover, it is easy to see that the derivative of $A_l(1, [v])$ is strictly smaller than the derivative of $A_e(1, [v])$, which proves

$$A_l(1, [v]) < A_e(1, [v])\,, \quad \text{for } R_{1[v]} < d_M \leq A_l([v], 0)\,, \tag{44}$$

meaning that $d_l(1, [v])$ is a point of H_2.

When instead $v = [v]$ and the vector d^R has only $[v]$ non zero entries equal to $R_{1[v]}$, we still set $d_M = R_{1[v]} + \zeta$, but choosing $0 < \zeta \leq A_l([v]-1,0) - R_{1[v]}$. By repeating the previous argument, we get the admissible vector $d_l(1,[v]-1)$ such that $A_l(1,[v]-1) < A_e(1,[v]-1)$. We note that, as $v \neq 1$ by hypothesis, $d_l(1,[v]-1)$ is well defined. Thus, for any $R_{1[v]} < d_M \leq A_l([v]-1,0)$, $d_l(1,[v]-1)$ belongs to H_2, which is then non-empty.

Coming to point iii), we start proving that $H_3 = \emptyset$ for $v = n$. Each vector of H_3 satisfies the inequalities (28) as well as Cauchy-Schwartz inequality $n\sum_{k=1}^n d_k^2 \geq (\sum_{k=1}^n d_k)^2$. Then, for $v = n$ (and thus $S^2 = nQ$), points of H_3 should simultaneously satisfy

$$nQ > n\sum_{k=1}^{n} d_k^2 \geq \left(\sum_{k=1}^{n} d_k\right)^2 > S^2\,,$$

which is absurd.

Let us now consider $v \neq n$. To demonstrate that $d_M \leq A_e(n,0)$ implies $H_3 = \emptyset$, let us consider the optimization problem

$$\min_{d\in\Omega_3} d_n, \tag{45}$$

with

$$\Omega_3 = \{d \in \mathbb{R}^n : g_e(n,d) = 0,\, g_l(n,d) < 0\,,\, d_n \geq d_{n-1} \geq \ldots \geq d_1 \geq 0\}\,. \tag{46}$$

Recalling that in view of (34), $A_e(n,0) = \min\{A_e(n,0), A_l(n,0)\}$ and following the procedure adopted for the similar problems in (39), (42), we obtained the minimum point $d_e(n,0)$ which proves the implication $\{H_3 \neq \emptyset \Rightarrow d_M \geq A_e(n,0)\}$. The inverse implication $\{d_M \geq A_e(n,0) \Rightarrow H_3 \neq \emptyset\}$ of point iii) is verified as the vector having elements $d_k = A_e(n,0), k = 1,\ldots,n$, belongs to H_3 by its very definition.

In view of (35) and (40), it is $A_e(n,0) \leq R_{1[v]}$ and, collecting the results obtained so far for points i)-iii), we conclude that for $d_M < A_e(n,0)$ the sets $H_i, i = 1,2,3$ are empty and the optimal solution must belong to H_4.

Finally, the non-emptiness of H_4 for any d_M is guaranteed by the existence of the trivial null vector: $d_k = 0, k = 1,\ldots,n$. ∎

Lemma 3.2. *For $k_e(n) - k_l > 0$, $\rho_e k_l - \rho_l k_e(n) > 0$, and $1 \leq v \leq n$ the optimal solution changes as d_M and ρ change, and it belongs to the sets* (21) *according to the following Tables 2–4.*

Table 2: Sets of (21) containing the optimal solution for $1 < v < n$.

d_M	$\left(0, A_e(n,0)\right)$	$\left[A_e(n,0), R_{1[v]}\right)$	$R_{1[v]}$	$\left(R_{1[v]}, \infty\right)$
$\rho < \rho_l$	H_4	H_3	H_1	H_2
$\rho = \rho_l$	H_4	H_3	H_1	$H_1 \cup H_2$
$\rho_l < \rho < \rho_e$	H_4	H_3	H_1	H_1
$\rho = \rho_e$	H_4	H_3	$H_1 \cup H_3$	$H_1 \cup H_3$
$\rho > \rho_e$	H_4	H_3	H_3	H_3

Table 3: Sets of (21) containing the optimal solution for $v = 1$.

d_M	$\left(0, A_e(n,0)\right)$	$\left[A_e(n,0), R_{1[v]}\right)$	$\left[R_{1[v]}, \infty\right)$
$\rho < \rho_e$	H_4	H_3	H_1
$\rho = \rho_e$	H_4	H_3	$H_1 \cup H_3$
$\rho > \rho_e$	H_4	H_3	H_3

Table 4: Sets of (21) containing the optimal solution for $v = n$.

d_M	$\left(0, A_l(n,0)\right)$	$A_l(n,0) \equiv R_{1[v]}$	$\left(R_{1[v]}, \infty\right)$
$\rho < \rho_l$	H_4	H_1	H_2
$\rho = \rho_l$	H_4	H_1	$H_1 \cup H_2$
$\rho > \rho_l$	H_4	H_1	H_1

Proof. The first column of Tables 2–4 for $d_M < A_e(n,0)$ is directly obtained from Property 1. In Table 4, being $v = n$, it is $A_e(n,0) = A_l(n,0)$.

For $d_M \geq A_e(n,0)$, the optimum belongs to $H_1 \cup H_2 \cup H_3$ and the proof is based on the comparison of the values taken by the cost function within the sets H_1, H_2, and H_3, supposing initially that they are all non-empty and then verifying their actual non-emptiness, which depends on the limiting value d_M (Lemma 3.1).

We begin observing that all the points of H_1 enjoy the properties (25) and (26), so that they all give the same constant value of $J_n(d)$, here denoted by C_1:

$$J_n(d)|_{d\in H_1} \triangleq C_1 = -k_e(n)\frac{\rho - \rho_l}{\rho_e - \rho_l} - k_l\frac{\rho_e - \rho}{\rho_e - \rho_l}\,. \tag{47}$$

Concerning $J_n(d)$ in H_2 and H_3, when the equality provided by the late, or respectively early, constraint is imposed, the cost function becomes a function of $s \triangleq \sum_{k=1}^{n} d_k$ only. Let us denote by C_2, and respectively C_3, the functions so obtained in H_2 and H_3. We have

$$J_n(d)|_{d\in H_2} \triangleq C_2(s) = -k_l + (\rho_l - \rho)s\,, \quad s < S\,, \tag{48}$$

and

$$J_n(d)|_{d\in H_3} \triangleq C_3(s) = -k_e(n) + (\rho_e - \rho)s\,, \quad s > S\,, \tag{49}$$

where the definition intervals of s derive from the constraints (27) and (28), respectively holding in H_2 and in H_3. It can be seen that both the functions $C_2(s)$, $C_3(s)$ tend to the same value C_1, i.e. the value of the cost function in H_1, for a total dose $s \to S$. So, in order to select the optimum, the cost function provided by any candidate of H_2 or H_3 has to be compared to the constant C_1. Moreover, (48) and (49) show that the relative ordering among C_1, C_2 and C_3 depends on the sign of the differences $\rho_e - \rho$ and $\rho_l - \rho$.

Precisely, for $\rho < \rho_l$ (slowly proliferating tumours), both C_2 and C_3 are increasing functions of the total dose s and, for s in the appropriate intervals, it is

$$C_2(s) < C_1\,, \qquad C_1 < C_3(s)\,.$$

For tumours with $\rho > \rho_e$ (rapidly proliferating), both C_2 and C_3 are decreasing functions of the total dose and we have

$$C_3(s) < C_1\,, \qquad C_1 < C_2(s)\,.$$

When $\rho = \rho_l$ or $\rho = \rho_e$, we get limit conditions in which the LQ responses of tumour and normal tissue coincide. For $\rho = \rho_l$, any point of H_2 yields the same cost function value $C_2 = -k_l$, and we have $C_2 = C_1 < C_3(s)$. For $\rho = \rho_e$ any point of H_3 yields the same cost function value $C_3 = -k_e(n)$, with $C_3 = C_1 < C_2(s)$.

For tumours characterized by a radiosensitivity ratio such that $\rho_l < \rho < \rho_e$, C_2 decreases while C_3 increases with s. Then points of H_1 provide the minimum value of J_n, namely

$$C_1 < C_2(s)\,, \qquad C_1 < C_3(s)\,.$$

Merging the information about $J_n(d)$ related to ρ with the results of Lemma 3.1 about the value of d_M, we obtain the picture of the sets containing the optimal solution schematized in Table 2. Indeed, Lemma 3.1 states that for $d_M > R_{1[v]}$, H_1, H_2 and H_3 are all non-empty, for $d_M = R_{1[v]}$, H_1 and H_3 are non-empty, while for $d_M < R_{1[v]}$, only H_3, is non-empty. Therefore, when more than one set H_j $j = 1, 2, 3$, is non-empty, the ordering among the related C_j (dependent on the value of ρ) determines the set containing the optimum.

Tables 3 and 4, respectively referring to $v = 1$ and $v = n$ can be obtained in a similar way taking into account Lemma 3.1 and the ordering relations among the cost function values in the sets (21). ∎

The following theorem establishes, by selecting the minimum-cost vector within the sets identified by means of Lemma 3.2 (Tables 2–4), the optimal solution as a function of ρ and d_M, in the absence of a prevalent normal tissue constraint.

Theorem 3.3. *For $k_e(n) - k_l > 0$, $\rho_e k_l - \rho_l k_e(n) > 0$, and $1 \le v \le n$, the optimal solutions of Problem 2.2 in terms of ρ and d_M are reported in Tables 5a–5c.*

Proof. Let us begin by deriving Table 5a from Table 2 for $1 < v < n$. The optima in the first column come directly from Property 1, which states that the unique optimal solution for $d_M < A_e(n, 0)$ is $\tilde{d}$, with $d_k = d_M$, $k = 1, \ldots, n$.

It is also rather simple to assess the optimal solutions for $\rho_l \le \rho < \rho_e$, $d_M \ge R_{1[v]}$ and for $\rho = \rho_e$, $d_M \ge A_e(n, 0)$. Indeed, as seen in Property 2, when $\rho_l \le \rho \le \rho_e$ the system of KKT conditions admits an infinite set of solutions all cost-equivalent. The definition of this infinite set, which depends on ρ, is the following: H_1 for $\rho_l < \rho < \rho_e$, $H_1 \cup H_2$ for $\rho = \rho_l$, and $H_1 \cup H_3$ for $\rho = \rho_e$. The non-emptiness of these sets, for the values of d_M mentioned above, is guaranteed by Lemma 3.1. Furthermore, as proved in Lemma 3.2, all the points of these solution sets result in the lowest cost function value, compared to other possible admissible points. So, for d_M decreasing, as long as each solution set does not reduce to the empty set, the optimum can be chosen arbitrarily, and we adopt the choice of selecting the candidate surviving for the largest interval of d_M values. In particular, we select the following representative optimal solutions: i) for $\rho_l \le \rho < \rho_e$ (second

Table 5: Optimal solutions $d_n^\star$ with respect to the tumour parameter ρ and to the value of d_M. Table 5a, $1 < v < n$. The columns with headings containing additional conditions on v exist only for the specified values. Optima of items such that $\rho_l \leq \rho < \rho_e$, $d_M \geq R_{1[v]}$, and $\rho = \rho_e$ are representative optimal vectors. Table 5b, $v = 1$. Row $\rho = \rho_e$ reports representative optimal vectors. Table 5c, $v = n$. Row $\rho = \rho_l$ reports representative optimal vectors.

(a)

d_M	$\big(0, A_e(n,0)\big)$	$\big[A_e(u+1,0), A_e(u,0)\big)$ $[v]+1 \leq u \leq n-1$	$\big[A_e([v]+1,0), R_{1[v]}\big)$	$R_{1[v]}$	$\big(R_{1[v]}, A_l([v],0)\big]$	$\big(A_l(u+1,0), A_l(u,0)\big]$ $1 \leq u \leq [v]-1$	$\big(A_l(1,0), \infty\big)$
v		$< n-1$			$\neq [v]$	> 2	
$\rho<\rho_l$	$\tilde{d}$	$d_e(1,u)$	$d_e(1,[v])$	d^R	$d_l(1,[v])$	$d_l(1,u)$	$d_l(1,0)$
$\rho=\rho_l$	$\tilde{d}$	$d_e(1,u)$	$d_e(1,[v])$	d^R	d^R	d^R	d^R
$\rho_l<\rho<\rho_e$	$\tilde{d}$	$d_e(1,u)$	$d_e(1,[v])$	d^R	d^R	d^R	d^R
$\rho=\rho_e$	$\tilde{d}$	$d_e(n,0)$	$d_e(n,0)$	$d_e(n,0)$	$d_e(n,0)$	$d_e(n,0)$	$d_e(n,0)$
$\rho>\rho_e$	$\tilde{d}$	$d_e(n,0)$	$d_e(n,0)$	$d_e(n,0)$	$d_e(n,0)$	$d_e(n,0)$	$d_e(n,0)$

(b)

d_M	$\big(0, A_e(n,0)\big)$	$\big[A_e(u+1,0), A_e(u,0)\big)$ $1 \leq u \leq n-1$	$\big[A_e(1,0), \infty\big)$
$\rho<\rho_e$	$\tilde{d}$	$d_e(1,u)$	$d_e(1,0)$
$\rho=\rho_e$	$\tilde{d}$	$d_e(n,0)$	$d_e(n,0)$
$\rho>\rho_e$	$\tilde{d}$	$d_e(n,0)$	$d_e(n,0)$

(c)

d_M	$\big(0, A_l(n,0)\big)$	$\big[A_l(u+1,0), A_l(u,0)\big)$ $1 \leq u \leq n-1$	$\big[A_l(1,0), \infty\big)$
$\rho<\rho_l$	$\tilde{d}$	$d_l(1,u)$	$d_l(1,0)$
$\rho=\rho_l$	$\tilde{d}$	$d_l(n,0)$	$d_l(n,0)$
$\rho>\rho_l$	$\tilde{d}$	$d_l(n,0)$	$d_l(n,0)$

and third row) and $d_M \geq R_{1[v]}$, the vector $d_R \in H_1$; ii) for $\rho = \rho_e$ and $d_M \geq A_e(n,0)$, the vector $d_e(n,0)$.

Going to all the remaining values of ρ and d_M in Table 2, still on the basis of Property 2, only structured solutions, either of the kind $d_e(i,j) \in H_3$, or $d_l(i,j) \in H_2$, or $d_e(i,j) \equiv d_l(i,j) \in H_1$, can exist. Then, for $d_M \geq A_e(n,0)$, the optimum changes as d_M takes values in the intervals delimited by the values (34) plus $R_{1[v]}$, which are ordered according to (35) and (40). Therefore, the last three columns of Table 2 have been split accordingly in Table 5a. The 3rd and 7th column are possibly multiple columns to be repeated or omitted depending on the value of v, as indicated in the table.

When only structured candidates exist, to determine the optimum it suffices to compare the cost function values over a finite set of discrete solutions, taking into account the cost function expressions (47)–(49). While $J_n(d)$ is constant in H_1, (48), (49) show that the cost function is a (linear) function of the sum s of the dose fractions, either increasing or decreasing depending on ρ. The minimal cost function is then given by vectors with minimal s when J increases, and by points with maximal s otherwise.

Among the totality of the structures $d_e(i,j)$, $d_l(i,j)$ (not simultaneously acceptable, unless $d_e(i,j) = d_l(i,j)$), with $i = 1,\ldots,n$, $j = 0,\ldots,n-i$, we are now interested in determining the subset of indexes i,j such that $\min\{A_e(i,j)\,,\ A_l(i,j)\} \in [0, d_M]$.

To this aim, let d_M belong to one of the intervals identified by the n minima in (34). Without specifying if such minima are "early" or "late" values, we prove what follows.

If

$$d_M \in \Big(\min\{A_e(u+1,0), A_l(u+1,0)\},\, \min\{A_e(u,0), A_l(u,0)\}\Big)\,, \quad u = 1,\ldots,n-1\,, \tag{50}$$

only the structured vectors, $d_e(i,j)$ or $d_l(i,j)$, with

$$j = 0,\ldots,u\,,\ i = u+1-j,\ldots,n-j\,, \tag{51}$$

have entries in $[0, d_M]$.

In order to prove (51), we need to preliminary settle some properties holding for both $A_e(i,j)$, $A_l(i,j)$. Without loss of generality, we consider the values $A_e(i,j)$. We have

$$d_M \leq A_e(m,0) \quad \Leftrightarrow \quad A_e(i,j) \geq 0\,, \qquad j = m\,, \tag{52}$$

for any index $m = 1,\ldots,n-1$, and

$$d_M \geq A_e(h,0) \quad \Leftrightarrow \quad A_e(i,j) \leq d_M\,, \qquad i+j = h\,, \tag{53}$$

for any $h = 1,\ldots,n$. Noting that the inequality $d_M \leq A_e(m,0)$ coincides with $m d_M^2 + m\rho_e d_M - k_e \leq 0$, while $d_M \geq A_e(h,0)$ coincides with $h d_M^2 + h\rho_e d_M - k_e \geq 0$, (52) can be proved starting from the equation that defines $A_e(i,j)$:

$$i A_e^2(i,j) + i\rho_e A_e(i,j) + j d_M^2 + j\rho_e d_M - k_e = 0\,. \tag{54}$$

In fact, if $d_M \leq A_e(m,0)$, setting $j = m$ in (54) we obtain $A_e(i,m) \geq 0$, for any i. Conversely, given a pair i, j such that $j = m$ and $A_e(i,j) \geq 0$, from equation (54) we obtain $m d_M^2 + m\rho_e d_M - k_e \leq 0$, so that $d_M \leq A_e(m,0)$.

To prove property (53), we rewrite (54) for $j = h - i$ and, taking into account that $hd_M^2 + h\rho_e d_M - k_e \geq 0$, we obtain

$$i\,(d_M + A_e(i,j) + \rho_e)\,(A_e(i,j) - d_M) \leq 0\,, \quad i + j = h\,, \tag{55}$$

which, being $(d_M + A_e(i,j) + \rho_e) > 0$, implies $A_e(i,j) \leq d_M$ for any admissible pair i, j such that $i + j = h$. Moreover, from (54), given i, j such that $i + j = h$ and $A_e(i,j) \leq d_M$, the inequality $d_M \geq A_e(h,0)$ follows.

Since $A_e(i,0)$ decreases as i increases (see (30)), property (53) implies the following admissibility condition for $A_e(i,j)$:

$$d_M \geq A_e(h,0) \quad \Rightarrow \quad A_e(i,j) \leq d_M\,, \qquad h \leq i + j \leq n\,, \tag{56}$$

while (52) implies

$$d_M \leq A_e(m,0) \quad \Rightarrow \quad A_e(i,j) \geq 0\,, \qquad 1 \leq j \leq m\,, \tag{57}$$

which, being $A_e(i,0)$ positive by definition, can be extended including $j = 0$ becoming

$$d_M \leq A_e(m,0) \quad \Rightarrow \quad A_e(i,j) \geq 0\,, \qquad 0 \leq j \leq m\,. \tag{58}$$

From (52), (53), also the opposite conditions about the non-admissibility of $A_e(i,j)$ can be derived:

$$d_M < A_e(h,0) \quad \Rightarrow \quad A_e(i,j) > d_M\,, \qquad 1 \leq i + j \leq h\,, \tag{59}$$

$$d_M > A_e(m,0) \quad \Rightarrow \quad A_e(i,j) < 0\,, \qquad m \leq j \leq n-1\,. \tag{60}$$

Now, we can prove that when d_M is chosen as in (50) for $u = 1, \ldots, n-1$, from properties (56)–(60) it follows $\min\{A_e(i,j), A_l(i,j)\} \in [0, d_M]$ for $j = 0, \ldots, u$, $i = u+1-j, \ldots, n-j$, while it follows $\min\{A_e(i,j), A_l(i,j)\} \notin [0, d_M]$ for all the remaining pairs i, j. This is equivalent to prove (51).

Let us denote by $A_p(u+1,0)$ and $A_P(u,0)$ the quantities $\min\{A_e(u+1,0), A_l(u+1,0)\}$ and respectively $\min\{A_e(u,0), A_l(u,0)\}$, where the subscripts p, P can be equal to 'e' or 'l', depending on being the minimum of 'e' or 'l' type (which in turn depends on the value of v in $(1,n)$). Let us similarly denote by $A_{\bar{p}}(u+1,0)$ and $A_{\bar{P}}(u,0)$ the quantities $\max\{A_e(u+1,0), A_l(u+1,0)\}$ and $\max\{A_e(u,0), A_l(u,0)\}$. Reminding that $1 \leq i + j \leq n$ and $0 \leq j \leq n-1$, in what follows we intend that a given property has to be disregarded whenever $i + j$ or j is out of its allowed range, as the related structure is missing.

Let us initially assume d_M within the open interval $(A_p(u+1,0), A_P(u,0))$. Then, it is $d_M < A_P(u,0) \leq A_{\bar{P}}(u,0)$, and (59) implies $A_e(i,j)$, $A_l(i,j) > d_M$, for $1 \leq i + j \leq u$, indicating that the related structures are not admissible. Moreover, (58) guarantees $A_e(i,j)$, $A_l(i,j) > 0$, for $j = 0, \ldots, u$. Furthermore, being $d_M > A_p(u+1,0)$, from (60) it results $A_p(i,j) < 0$, for $j = u+1, \ldots, n-1$, and the related structures have to be excluded. The structures $d_{\bar{p}}(i,j)$, with $j = u+1, \ldots, n-1$, have to be excluded as well, either directly, because $A_{\bar{p}}(i,j) < 0$, or because, being $A_{\bar{p}}(i,j) > 0 > A_p(i,j)$, they are not minimal. Exploiting again $d_M > A_p(u+1,0)$, from (56) it certainly is $A_p(i,j) < d_M$, for $u+1 \leq i + j \leq n$, but not necessarily $A_{\bar{p}}(i,j) < d_M$. Nevertheless, it is guaranteed that $\min\{A_p(i,j), A_{\bar{p}}(i,j)\} < d_M$, for $u+1 \leq i + j \leq n$.

Summarizing, it is $\min\{A_e(i,j), A_l(i,j)\} \in (0, d_M)$, for $j = 0, \ldots, u$, $i = u+1-j, \ldots, n-j$, whereas $\min\{A_e(i,j), A_l(i,j)\} \notin (0, d_M)$ for all the remaining indexes; then the vectors (51) are all (and only) the structured extremals.

The set of structured extremals is given by (51), even for $d_M = A_P(u,0)$. Since, it is $A_{\bar{P}}(u,0) \geq A_P(u,0) = d_M$, from (52), (53) we get $A_{\bar{P}}(i,j) \geq A_P(i,j) = d_M$ for $i+j=u$, and $A_{\bar{P}}(i,j) \geq A_P(i,j) = 0$ for $j=u$, which means that the structures $d_P(i,j)$ with $i+j=u$, and $d_P(i,j)$ with $j=u$, are extremals ($d_{\bar{P}}(i,j)$ can be extremal only when it coincides with $d_P(i,j)$ for the same index pair). Note that the vectors $d_P(i,j)$, with $i+j=u$, and the vectors $d_P(i,j)$, with $j=u$, are all equal to the vector having u entries equal to d_M and $n-u$ zeroes, so that it is unnecessary to explicitly include $d_P(i,j)$, with $i+j=u$, in the set (51). By means of a parallel argument, it can be seen that the index set (51) identifies all the structured extremals even for $d_M = A_p(u+1,0)$.

Linking together all the intervals in (50) for $u = 1,\ldots,n-1$, we get the total variability range of d_M, except the interval $(A_l(1,0),\infty)$. However, it is evident from (56) and (60) that for $d_M > A_l(1,0)$ only the structures with $j=0$, and precisely $d_l(i,0)$, $i=1,\ldots,[v]$ and $d_e(i,0)$, $i=\min\{[v]+1,\,n\},\ldots,n$, can be extremals. So, as it could be expected, setting $d_M > A_l(1,0)$, we find the same structured extremals found by Bertuzzi et al. (2013) for $n=5$ and in the absence of a dose upper bound.

The properties (56)–(60) define the (finite) set of indexes (51) identifying the only structured vectors, $d_e(i,j)$ or $d_l(i,j)$, that have entries in $[0,d_M]$, for $A_e(n,0) \leq d_M \leq A_l(1,0)$. We intend now to study the behaviour of the sum of the dose fractions, $s_e(i,j)$ or $s_l(i,j)$, related to $d_e(i,j)$ or $d_l(i,j)$, so as to show that the minimal total dose is attained for $i=1$, $j=u$, whereas the maximal for $i=n$, $j=0$. We refer, for instance, to $d_e(i,j)$.

Let us study the behaviour of $s_e(i,j)$ letting i vary and for a fixed j. Considering i as a continuous variable $z>0$, we have

$$s_e(z,j) = z\left(-\frac{\rho_e}{2} + \sqrt{\left(\frac{\rho_e}{2}\right)^2 + \frac{k_e(n) - j d_M(d_M+\rho_e)}{z}}\right) + j d_M\,, \tag{61}$$

which is physically meaningful for z such that $k_e - j d_M(d_M+\rho_e) > 0$ (namely $A_e(z,j)$ real and positive). Introducing the function

$$R(z) = \left(\frac{\rho_e}{2}\right)^2 + \frac{k_e(n) - j d_M(d_M+\rho_e)}{z}\,, \tag{62}$$

the derivative of (61) with respect to z is given by

$$\frac{\partial s_e(z,j)}{\partial z} = \frac{\left(\sqrt{R(z)} - \frac{\rho_e}{2}\right)^2}{2\sqrt{R(z)}}\,, \tag{63}$$

which is clearly non-negative.

Consider now the index $h = i+j$ in order to study the behaviour of $s_e(i,h-i)$ fixing h and letting i vary. As done before, we substitute i with a continuous variable $z>0$, so as to compute the derivative $\partial s_e(z,h-z)/\partial z$. It is easy to see that it is $\partial s_e(z,h-z)/\partial z \geq 0$. In summary, the total dose s_e is non-decreasing as i increases either for j fixed and for h fixed. Therefore, the minimal total dose is attained for the smallest i, namely $i=1$, which, from (51), is given by the largest j, i.e. $j=u$. The maximal total dose is given instead by the largest i that corresponds to the pair $i=n$ and $j=0$.

We can now examine the remaining parts of Table 5a. For $\rho > \rho_e$ and for any $d_M \geq A_e(n,0)$, the optimum belongs to H_3 and it is given by the vector with maximal sum of the doses, that

is $d_e(n,0)$. Indeed, we notice that, since $A_e(n,0) < A_l(n,0)$ in view of (34), the "early" vector $d_e(n,0)$ is actually admissible.

To complete the proof of Table 5a, it remains to examine three cases: i) $\rho < \rho_e$, $d_M < R_{1[v]}$; ii) $\rho < \rho_l$, $d_M > R_{1[v]}$; iii) $\rho < \rho_l$, $d_M = R_{1[v]}$. From Lemma 3.2 we know that the optima belong respectively to: i) H_3, ii) H_2 and iii) H_1. Concerning i), ii), since minimizing $C_3(s)$ for $\rho < \rho_e$ or minimizing $C_2(s)$ for $\rho < \rho_l$ is equivalent to minimize s (see (48), (49)), we must select the structured vector with the minimal s among the points of H_3 and, respectively, H_2. As seen above, the minimal s is provided by the pair $i = 1$, $j = 0, \ldots, n-1$, so the optimal solutions are: i) $d_e(1,u) \in H_3$, $u = [v], \ldots, n-1$; ii) $d_l(1,u) \in H_2$, $u = 0, \ldots, [v]$, provided they actually belong to H_3 and H_2, respectively. Let us then prove that the vector $d_e(1,u)$, $u = [v], \ldots, n-1$, belongs to H_3 by observing that in view of Lemma 3.1 the sets H_1, H_2 are empty for $d_M < R_{1[v]}$, and then it is $A_l(1,u) > d_M$, while in view of (50), (51) it is $0 \leq A_e(1,u) \leq d_M$. It follows $A_e(1,u) < A_l(1,u)$ which implies $d_e(1,u) \in H_3$, $u = [v], \ldots, n-1$. Next we prove $d_l(1,u) \in H_2$, $u = 0, \ldots, [v]$, by reminding that it is $s_l(1,0) < \ldots s_l([v],0) < S$ in view of (34) and (27). Recalling that $s_l(i, h-i)$ is a non-decreasing function of i with h fixed, setting $h = u+1$ and $i = 1, u+1$ we have $s_l(1,u) < s_l(u+1,0) < S$, which proves $d_l(1,u) \in H_2$, $u = 0, \ldots, [v]-1$. Moreover, $d_l(1,[v]) \in H_2$ is guaranteed by (44). Finally, we have to show that for $\rho < \rho_l$ and $d_M = R_{1[v]}$ the optimum is $d^R \in H_1$. The proof is immediate as d^R is the only vector of H_1 for $d_M = R_{1[v]}$ (see Appendix B for details).

The situations $v = 1$ and $v = n$ mean $d_e(1,0) \equiv d_l(1,0) \equiv d^R$ and, respectively, $d_e(n,0) \equiv d_l(n,0) \equiv d^R$. The related optimal solutions are reported in Tables 5b, 5c, which can be easily be obtained from Tables 3, 4 by the same argument used to derive Table 5a. ∎

Tables 5a–5c confirm the optimality of hypofractionated treatments for slowly proliferating tumours with $\rho < \rho_l$. In particular, if d_M is larger than $\min\{A_e(1,0), A_l(1,0)\}$, the optimal solution is unaffected by the dose upper bound and the optimal treatment consists of a single dose of radiation producing the whole maximal tolerable damage to normal tissues. Apart from some analytical interest, this solution is quite infeasible in practice, which provides a further "a posteriori" justification of the introduction of the upper bound d_M.

From a geometrical point of view, $v = 1$ means that the surfaces $g_e(n,d) = 0$ and $g_l(n,d) = 0$ are tangent in the point $d_l(1,0)$, while for $v = n$ they are tangent in $d_e(n,0)$. Except for the points of tangency, only points belonging to $g_e(n,d) = 0$ are admissible for $v = 1$, whereas only points on $g_l(n,d) = 0$ are admissible for $v = n$. Therefore, $v = 1$ and $v = n$ are in fact similar to the situation of prevalent early constraint and prevalent late constraint, respectively. Therefore, Tables 5b and 5c are still valid to represent the optimal solutions when one of the normal tissue constraints is prevalent on the other.

Because of the dependence of the repopulation term (and in particular of the maximal early damage $k_e(n)$) on the number n of fractions, the geometrical situation of a given radiotherapy problem can change as n changes, as we see in the next section.

A final observation can be made about the damage to normal tissues which, as it is known, can be reduced by spatially modulating the radiation intensity using suitable technological devices (Lee et al., 2006; Lu et al., 2008a,b). A suitable coefficient $f < 1$ accounting for the attenuation of the doses received by normal tissues can be included in the model and the problem constraints can be rewritten in terms of the portion of dose actually received by normal tissues, fd_k, $k = 1, ..., n$, with the effect of increasing ρ_e, ρ_l, $k_e(n)$, k_l, and d_M (Bertuzzi et al., 2013). Then, the optimal solutions turn out to be structurally identical to those of Tables 5a–5c with $f = 1$ but, with

respect to ρ, are characterized by a downward shift of the solution patterns as well as by larger fraction sizes.

4. Numerical simulation of the optimal solutions for variable n and determination of the optimal treatment time for specific tumour classes

Aim of this section is to determine by means of numerical simulations the optimal number of dose fractions, denoted by n°, the optimal vector d° of the fractionated dose, and the protocol duration $T(n^\circ)$ for the treatment of tumours having different proliferative behaviours - from fast to slow - and different radiosensitivities. After determinining the optimal solution $d_n^\star$ to Problem 2.2 for each n fixed ranging from 1 to n_M, the sequence $J^\star(n)$, $n = 1, \ldots, n_M$, is computed according to (17) in order to find the optimal number n° that provides the minimal value of the cost function.

The results of the current section are obtained assuming parameter values of the early and late normal tissues commonly found in the literature (Fowler et al., 2003a; Yang and Xing, 2005; Fowler, 2010). For the early responding normal tissue, we set $\rho_e = 10$ Gy, $\alpha_e = 0.35$ Gy^{-1}, $T_{Ke} = 7$ days and $T_{Pe} = 2.5$ days. As for the late normal tissue, the radiosensitivity ratio is set to $\rho_l = 3$ Gy, while the other parameters do not need to be specified, as the compensatory repopulation is negligible (Fowler, 2012).

We express the maximal tolerable damages to normal tissues by means of the Biologically Effective Dose (BED), a quantity originally introduced by Barendsen (1982), defined as the total radiation dose proportional to the logarithmic cell kill globally produced by a given reference protocol. Denoting by BED_e, BED_l the quantities related to the early and late reacting tissues respectively, the maximal tolerable damages to the normal tissues are given by $M_e = \alpha_e \mathrm{BED}_e$ and $M_l = \alpha_l \mathrm{BED}_l$, so that referring to conventional equi-fractionated protocols of the kind one fraction/day, five fractions/week, delivered in $\bar{n}$ fractions of size $\bar{d}$ over the time $\bar{T}$, we can write

$$M_e = \bar{n}\alpha_e \bar{d}\left(1 + \frac{\bar{d}}{\rho_e}\right) - \frac{\ln(2)}{T_{Pe}}(\bar{T} - T_{Ke})H(\bar{T} - T_{Ke}), \tag{64}$$

$$M_l = \bar{n}\alpha_l \bar{d}\left(1 + \frac{\bar{d}}{\rho_l}\right). \tag{65}$$

In view of (7) and (8), $k_e(n)$ and k_l are computed as

$$k_e(n) = \bar{n}\rho_e \bar{d}\left(1 + \frac{\bar{d}}{\rho_e}\right) - \frac{\ln(2)}{\beta_e T_{Pe}}\big(\bar{T} - T_{Ke}\big)H\big(\bar{T} - T_{Ke}\big) + \frac{\ln(2)}{\beta_e T_{Pe}}\big(T(n) - T_{Ke}\big)H\big(T(n) - T_{Ke}\big), \tag{66}$$

$$k_l = \bar{n}\rho_l \bar{d}\left(1 + \frac{\bar{d}}{\rho_l}\right). \tag{67}$$

Expression (66) shows that $k_e(n)$ is the sum of two parts: one independent of n attributable to the reference protocol, i.e. $\bar{k}_e = M_e/\beta_e$, and the other non-decreasing with n that accounts for the exponential regrowth occurring after T_{Ke}.

We stress that the dependence of $k_e(n)$ on n leads to changes in the geometry of the admissible domain, possibly modifying the relative prevalence of the normal tissue constraints according to Table 1. We also observe that, for any given reference protocol, it is $\mathrm{BED}_l > \mathrm{BED}_e$ and, being $k_e(\bar{n}) - k_l > 0$ with $k_e(n)$ non-decreasing, it is $k_e(n) - k_l > 0$ for any $n \geq \bar{n}$. The difference $\rho_e k_l - \rho_l k_e(n)$ is instead non-increasing with n and certainly positive for $1 \leq n \leq \bar{n}$, as it can be

easily seen from (66), (67). For reference protocols with $\bar{T} > T_{Ke}$, when n increases beyond $\bar{n}$ the quantity $\rho_e k_l - \rho_l k_e(n)$ decreases monotonically and it eventually becomes negative. Therefore, there exist a real value a, with $\bar{n} < a < +\infty$, such that $\rho_e k_l - \rho_l k_e(a) = 0$. For $n \geq a$, being $\rho_e k_l - \rho_l k_e(a) \leq 0$, any optimization problem with n fixed is going to be solved with prevalent late constraint (see Table 1).

As to the value of the daily upper bound, it is reasonable to assume $\bar{d} \leq d_M < \min\{\bar{A}_e(1,0), A_l(1,0)\}$, where $\bar{A}_e(1,0)$ is computed setting $k_e(n) = \bar{k}_e$ and $i = 1$ in (33). This condition guarantees the admissibility of the reference protocol and ensures optimal treatments consisting of at least two fractions.

Let us now consider the cost function $J^\star(n)$ defined by (17), recalling that, in view of (14)–(16), it is given by

$$J^\star(n) = J_n(d_n^\star) + E(n)\,, \tag{68}$$

where $d_n^\star$ is the optimal solution of Problem 2.2, which varies with the model parameters as depicted in Tables 5a–5c.

Below we give some properties of $J_n(d_n^\star)$ and $E(n)$ used in the following to prove the boundedness of the minimum point n° of $J^\star(n)$.

Property 4 For any pair ρ, d_M, and for $n \geq 1$, the functions $J_n(d_n^\star)$ and $E(n)$ enjoy the following properties:

1. $J_n(d_n^\star)$ is a negative, non-increasing function of n, i.e. $J_{n+1}(d_{n+1}^\star) \leq J_n(d_n^\star) < 0$;
2. $J_n(d_n^\star)$ has a finite lower bound;
3. $E(n)$ is a non-negative, non-decreasing function of n, i.e. $E(n+1) \geq E(n) \geq 0$;
4. $E(n) \geq \ln(2)((n-1)\Delta - T_K)/(\beta T_P)$, with $\Delta = 1$ day.

Consider the optimum $d_n^\star$ of the problem with dimension $n \geq 1$, denoting by $(d_n^\star)_k$ its entries for $k = 1, \ldots, n$. Point 1 can be derived by constructing the vector $d_{n+1}^\dagger$, with entries $(d_{n+1}^\dagger)_k = (d_n^\star)_k$, $k = 1, \ldots, n$ and $(d_{n+1}^\dagger)_{n+1} = 0$, and showing that it is an admissible vector, i.e. $d_{n+1}^\dagger \in D_{n+1}$. From the admissibility of the optimum $d_n^\star$, taking into account $k_e(n+1) \geq k_e(n) > 0$ and the identities $\sum_{k=1}^{n}(d_n^\star)_k \equiv \sum_{k=1}^{n+1}(d_{n+1}^\dagger)_k$, $\sum_{k=1}^{n}(d_n^\star)_k^2 \equiv \sum_{k=1}^{n+1}(d_{n+1}^\dagger)_k^2$, we get

$$\begin{aligned}
&\rho_e \sum_{k=1}^{n+1}(d_{n+1}^\dagger)_k + \sum_{k=1}^{n+1}(d_{n+1}^\dagger)_k^2 - k_e(n+1) \leq \rho_e \sum_{k=1}^{n}(d_n^\star)_k + \sum_{k=1}^{n}(d_n^\star)_k^2 - k_e(n) \leq 0,\\
&\rho_l \sum_{k=1}^{n+1}(d_{n+1}^\dagger)_k + \sum_{k=1}^{n+1}(d_{n+1}^\dagger)_k^2 - k_l = \rho_l \sum_{k=1}^{n}(d_n^\star)_k + \sum_{k=1}^{n}(d_n^\star)_k^2 - k_l \leq 0,\\
&0 \leq (d_{n+1}^\dagger)_k \leq d_M,\ k = 1, \ldots, n+1,
\end{aligned} \tag{69}$$

which imply $d_{n+1}^\dagger \in D_{n+1}$. Thus, from the very definition of $d_{n+1}^\star$, which is the optimum of the problem with dimension $n+1$, we have

$$J_{n+1}(d_{n+1}^\star) \leq J_{n+1}(d_{n+1}^\dagger) \equiv J_n(d_n^\star)\,. \tag{70}$$

Finally, the negativity of $J_n(d_n^\star)$ for $n = 1$ guarantees $J_n(d_n^\star) < 0$ for $n > 1$.

As seen above, for $n \geq a$ the late constraint is prevalent and the optimal solutions necessarily satisfy the constraint $g_l(n, d_n^\star) = 0$. According to Table 5c, for $\rho < \rho_l$, the optimum is $d_n^\star = d_l(1, u)$, where u is independent of n and, for any given d_M, it is identified by the relationship $A_l(u+1, 0) \leq d_M < A_l(u, 0)$. Moreover, u must be strictly smaller than $\bar{n}$, since it is $d_M \geq A_l(\bar{n}, 0) = A_e(\bar{n}, 0) = \bar{d}$. For $\rho \geq \rho_l$, the optimal vector is $d_n^\star = d_l(n, 0)$. So, for $n \geq a$, exploiting the relation $\sum_{k=1}^{n}(d_n^\star)_k^2 = -k_l + \rho_l \sum_{k=1}^{n}(d_n^\star)_k$, we have

$$J_n(d_n^\star) = \begin{cases} -k_l - (\rho - \rho_l)(A_l(1, u) + u d_M)\,, & \rho < \rho_l\,, \quad u \text{ s.t. } A_l(u+1, 0) \leq d_M < A_l(u, 0)\,, \\ -k_l - (\rho - \rho_l) n A_l(n, 0), & \rho \geq \rho_l\,. \end{cases} \tag{71}$$

It can be noticed that, when $\rho < \rho_l$, $J_n(d_n^\star)$ is constant for $n \geq a$. In view of point 1, the constant value in (71) constitutes the sought lower bound of $J_n(d_n^\star)$ for any $n \geq 1$. Concerning $\rho \geq \rho_l$, substituting the expression of $A_l(n, 0)$ (see (33) with $i = n$) in Eq. (71), it can be easily verified that $J_n(d_n^\star)$ is a decreasing function of n, which, for n increasing, tends to the finite limit $-\rho k_l/\rho_l$. So, as a consequence of point 1, the value $-\rho k_l/\rho_l$ is a lower bound for $J_n(d_n^\star)$, for $n \geq 1$.

Item 3 derives from the definition of $T(n)$ in (2) and from the Heaviside function definition. Indeed, we have

$$E(n) = \begin{cases} 0, & \text{for } T(n) \leq T_K, \\ \dfrac{\ln(2)}{\beta T_P}\big(T(n) - T_K\big), & \text{for } T(n) > T_K. \end{cases}$$

Since from Eq. (2) it is $T(n+1) > T(n)$, we get $E(n) = 0$ for n such that $T(n) \leq T_K$ and $E(n+1) > E(n) > 0$ otherwise. Finally, provided that T_K is finite, the inequality $T(n) \geq (n-1)\Delta$ implies

$$E(n) \geq \frac{\ln(2)}{\beta T_P}\big(T(n) - T_K\big) \geq \frac{\ln(2)}{\beta T_P}\big((n-1)\Delta - T_K\big)\,.$$

∎

Property 4 allows us to establish the boundedness of the optimal number of fraction n° for any tumour type. In the following, n_K denotes the number of fractions that can be delivered during the time T_K according to the scheme one fraction/day, five fractions/week, i.e. n_K denotes the integer such that $T(n_K) \leq T_K < T(n_K + 1)$.

Remark 4.1. *The minimum point n° of the function* (68) *on the open interval $n \geq 1$ exists and it is finite both for $\rho \geq \rho_l$ and for $\rho < \rho_l$. Based on Property 4, for $\rho \geq \rho_l$, we have*

$$J^\star(n) > -\frac{\rho k_l}{\rho_l} + \frac{\ln(2)}{\beta T_P}[(n-1)\Delta - T_K]\,. \tag{72}$$

Let us now note that, if tumour repopulation occurs at a finite time T_K, the right hand side of (72) *is an increasing function of n and let us denote by $\tilde{n}$ the real value at which it vanishes. We have*

$$\tilde{n} = \frac{1}{\ln(2)}\frac{\alpha k_l}{\rho_l}\frac{T_P}{\Delta} + \frac{T_K}{\Delta} + 1\,, \tag{73}$$

which is clearly finite. Therefore, since $J^\star(n)$ is negative and non-increasing until the onset of repopulation, that is for $T(n) \leq T_K$, while it is positive for $n \geq \tilde{n}$, the function $J^\star(n)$ attains its minimum at n° such that $n_K \leq n^\circ < \tilde{n}$.

In the presence of accelerated tumour repopulation, the optimal treatment time $T(n^\circ)$ must be greater than, or at least equal to, T_K. Therefore, in the numerical simulations we choose n_M such that $T(n_M) > T_K$, based on literature indications about the value of T_K. Indeed, if n_M were chosen such that $T(n_M) \leq T_K$, we would get a trivial optimum $n^\circ = n_M$.

For tumours having $\rho < \rho_l$, even in the absence of tumour repopulation, the optimal number of fraction doses n° is limited by the value a defined by $\rho_e k_l - \rho_l k_e(a) = 0$. In fact, unlike the previous case, the dose dependent term of $J^\star(n)$ remains constant and equal to its lower limit for $n \geq a$, i.e. $J_n(d_n^\star) = -k_l - (\rho - \rho_l)(A_l(1,u) + u d_M)$ with u the fixed integer such that $A_l(u+1,0) \leq d_M < A_l(u,0)$. As $J^\star(n)$ cannot decrease for $n \geq a$, it must attain its minimum at n° such that $n^\circ \leq a$.

In the following remark, we further examine some properties of the normal tissue constraints in order to extend to $n \geq \bar{n}$ the interval in which the optimal solution lies on the late constraint boundary.

Remark 4.2. *It is possible to find a sufficient condition, involving the normal tissue parameters, that guarantees that the late constraint is the most restrictive constraint even for $\bar{n} < n < a$. Since in the mentioned interval of n, it is $k_e(n) - k_l > 0$ and $\rho_e k_l - \rho_l k_e(n) > 0$, it suffices to find a condition implying that the global parameter v (defined in (19)) satisfies $v > n$. Indeed, for n such that $T(n) > T_{Ke}$ and $n < a$, v is positive and equal to*

$$v = \frac{[(\rho_e - \rho_l)\bar{n}\bar{d} + \ln(2)(T(n) - \bar{T})/(\beta_e T_{Pe})]^2}{(\rho_e - \rho_l)[(\rho_e - \rho_l)\bar{n}\bar{d}^2 - \rho_l \ln(2)(T(n) - \bar{T})/(\beta_e T_{Pe})]} = \frac{\bar{n}[1 + c(T(n) - \bar{T})]^2}{[1 - \frac{\rho_l}{\bar{d}} c(T(n) - \bar{T})]}\,, \tag{74}$$

where

$$c = \frac{\ln(2)}{\beta_e T_{Pe}(\rho_e - \rho_l)\bar{n}\bar{d}} > 0\,.$$

First of all, from (74) it is easy to see that for $n = \bar{n}$ it is $v = \bar{n}$, which implies that $d_n^\star$ belongs to the late constraint boundary even for $n = \bar{n}$ (see Theorem 3.3). Moreover, it can be proved that if $2\bar{n}c \geq 1$, it is $v > n$ for $\bar{n} < n < a$. This can be done, for instance, by substituting to n a continuous variable z, computing the derivative of v with respect to z, and verifying that it is greater than 1 in the mentioned interval of n. Thus, recalling the expression of c, we can write the following condition sufficient to guarantee $v > n$ for $\bar{n} < n < a$:

$$\frac{2\ln(2)}{\beta_e T_{Pe}(\rho_e - \rho_l)\bar{d}} \geq 1\,. \tag{75}$$

In summary, under the condition (75), all the optimization problems with $n \geq \bar{n}$ are characterized by an optimal solution $d_n^\star$ satisfying $g_l(n, d_n^\star) = 0$ (as in Table 5c). Therefore, the function $J_n(d_n^\star)$ is defined as in (71) even for $n \geq \bar{n}$, with $\bar{n} < a$. As a consequence, for tumours having $\rho < \rho_l$, $J_n(d_n^\star)$ equals its lower bound for $n \geq \bar{n}$, which implies that the optimal number of fraction doses n° is now limited by the number of fraction doses of the reference protocol $\bar{n}$. In other words, if condition (75) holds, hypofractionated protocols shorter than the reference protocol are expected to be optimal for slowly proliferating tumours. We finally observe that the parameter values chosen to perform the following numerical simulations are such that the sufficient condition (75) is fulfilled.

To quantify the maximal admissible damages to normal tissues, as well as to rate possible advantages obtainable by our optimal schedules, we choose as a reference protocol one of the

protocols most commonly used for the clinical treatment of fast proliferating tumours, namely the "strong standard" fractionation schedule $35\,\mathrm{F} \times 2\,\mathrm{Gy} = 70\,\mathrm{Gy}/46$ days. Setting $\bar{n} = 35$, $\bar{d} = 2$ Gy, $\bar{T} = 46$ days, we get $\mathrm{BED}_l = 116.7$ Gy, $\mathrm{BED}_e = 53.1$ Gy (Fowler, 2008; Yang and Xing, 2005), and then $k_l = 350$ Gy^2, $\bar{k}_e = 531.05$ Gy^2.

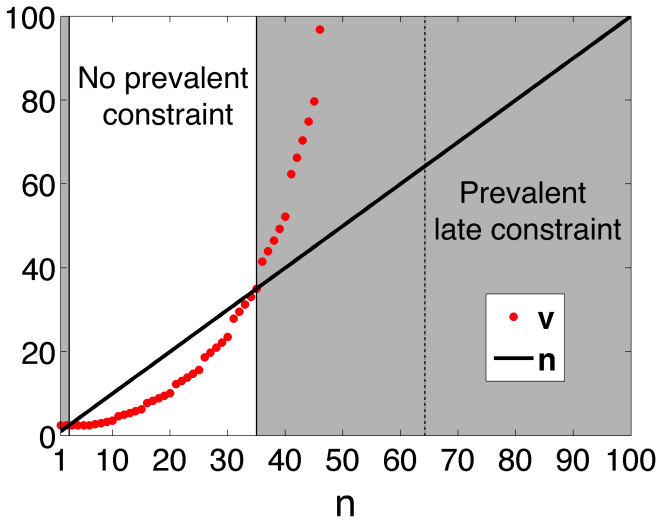

Figure 1: Global parameter v as a function of n and consequent geometry of the admissible domain. The quantity v is computed as in (74) for $n \in [1, 100]$ with normal tissue parameters given in the text and for the "strong standard" reference protocol.

Fig. 1 illustrates the plot of v for $n \in [1, 100]$, for the assumed healthy tissue parameters and the chosen reference protocol, evidencing the changes with n in the geometry of the admissible domain. As stated above, for $n \geq \bar{n}$, the whole sequence of optimal solutions for n fixed belongs to the boundary of the late constraint (Table 5c), and in our parameter setting, the vertical asymptote of v is at $a = 64.23$. For $n \in [3, 34]$, it is $1 < v < n$, so that none of the normal tissue constraints is prevalent and the optimal solution for each n can be found in Table 5a.

The admissible domain for each n is obviously trimmed by the daily upper bound, d_M, and since one purpose of these simulations is to compare the obtained optima to real radiotherapy protocols, we selected some values of d_M following the clinical literature, especially relevant to prostate cancer. Precisely, we set d_M to 3 Gy (Ritter et al., 2009), 5 Gy (Menkarios et al., 2011), 6 Gy (Collins et al., 1991), and 7 Gy (Tang et al., 2008). We observe that the chosen d_M values satisfy $\bar{d} \leq d_M < \min\{\bar{A}_e(1, 0), A_l(1, 0)\}$.

In the following, we focus on three cumulative tumour classes identified by the radiosensitivity ratio intervals $\rho < \rho_l$, $\rho_l \leq \rho < \rho_e$, and $\rho \geq \rho_e$. Note that, with the choice of the representative optimal solutions made in Tables 5a–5c, the limit cases $\rho = \rho_e$ and $\rho = \rho_l$ can be merged into the open intervals $\rho_l < \rho < \rho_e$ and $\rho > \rho_e$, respectively. For a given tumour class, the repopulation parameters are set according to indications coming from the literature, both experimental and theoretical. Furthermore, we investigate how changes of the tumour parameters affect the optimal solutions.

The procedure adopted to determine the optimal solutions is the same in all the next subsections and it is structured as follows:

1. set the normal tissue parameters ρ_e, α_e, T_{Ke}, T_{Pe}, and ρ_l (as indicated above in the text);
2. fix a tumour class setting the radiosensitivity and repopulation parameters ρ, α, T_P, T_K;
3. select a clinical radiotherapy protocol ($\bar{n}\,\mathrm{F}\times\bar{d}\,\mathrm{Gy} = \bar{n}\bar{d}\,\mathrm{Gy}/\bar{T}$ days) as the reference protocol in order to compute the maximal tolerable damages M_e, M_l through (64), (65);
4. set the daily dose upper bound d_M, with $\bar{d} \le d_M < \min\{\bar{A}_e(1,0), A_l(1,0)\}$;
5. for each $n = 1, \ldots, n_M$
   (a) compute $k_e(n)$, k_l from (66), (67) and v from (19);
   (b) compute $R_{1[v]}$ in (36), and the quantities in (34);
   (c) select the optimal solution $d_n^\star$ from Tables 5a–5c and compute the related $J^\star(n) = J(n, d_n^\star)$;
6. pick out the optimal fraction number n° providing the minimum among the values $J^\star(n)$ in $\{1, \ldots, n_M\}$;
7. calculate the optimal treatment length $T(n^\circ)$ from (2).

It is interesting to compare the effect of the optimal protocols so obtained to the effect produced by real clinical schedules taken from the literature. The comparison among protocols is often based on the "log cell kill", a quantity proportional to our cost function, commonly used to evaluate the tumour damages induced by radiation treatments. The log cell kill (LCK) is defined as

$$\log_{10}\left(\frac{1}{S}\right) = \alpha\,\log_{10}(\mathrm{e})\left[\sum_{k=1}^{n} d_k + \frac{1}{\rho}\sum_{k=1}^{n} d_k^2 - \frac{\ln(2)}{\alpha T_P}(T(n) - T_K)H(T(n) - T_K)\right]. \qquad (76)$$

We incidentally observe that minimizing $J^\star(n)$ with respect to n is equivalent to maximizing the quantity in square brackets in (76).

4.1. Fast proliferating tumours

Rapidly proliferating tumours are characterized by relatively high radiosensitivity ratios (Fowler, 2012) that we locate in the range $\rho \ge \rho_e$. Collecting the results of Tables 5a–5c related to this case, we see that, for any given n, the optimal protocol is uniformly fractionated and made of n equal non-zero doses given by $\min\{A_e(n,0), A_l(n,0), d_M\}$, where the item being the minimum depends on the constraint geometry for that n. The optimality of equi-fractionated protocols and the analytical expression of the dose fraction for the treatment of tumours of this class have been reported by many authors, see for instance Mizuta et al. (2012); Saberian et al. (2015); Badri et al. (2016).

Most human tumours are reckoned to belong to the class of fast proliferating tumours, like for instance head and neck, lung and cervical cancers (Thames et al., 1990; Qi et al., 2006; Fowler, 2012; Oliveira et al., 2012; Halperin et al., 2013). Thus, indications about the parameter values coming from the literature are widespread, and unavoidably the estimates are highly uncertain. For the numerical simulations, we select a "nominal" set of parameter values, related to head and neck cancer, as the most recurrent in the literature: $\rho = 10$ Gy, $\alpha = 0.35$ Gy^{-1}, $T_K = 21$ days, $T_P = 3$ days (e.g. Fowler (2007)). Then, to illustrate our procedure evaluating the sensitivity of

the optimal solutions to variations of the parameter values, still following the literature, we focus on the parameter intervals: $\rho = 10 \div 50$ Gy, $\alpha = 0.2 \div 0.5$ Gy^{-1}, $T_K = 7 \div 28$ days, $T_P = 1 \div 9$ days.

In the first example we assume the nominal parameter set. For these values, the standard protocol yields a tumour log cell kill equal to 9.55. Moreover, we set $n_M = 100$ for the computation of the sequence $J^\star(n)$. As long as $d_M \geq \bar{d}$, the optimal number of fractions is $n^\circ = 35$ with optimal fraction size 2 Gy and optimal treatment time 46 days. Therefore, the resulting optimal protocol coincides with the chosen reference protocol. This basic example allows us to highlight some

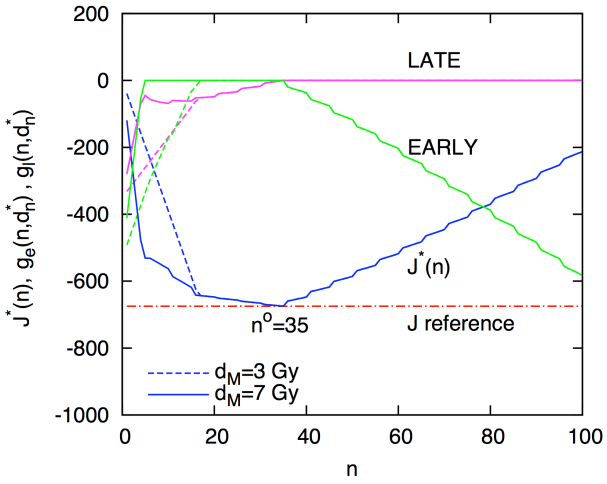

Figure 2: Profiles of $J^\star(n)$, $g_e(n, d_n^\star)$, and $g_l(n, d_n^\star)$ for fast proliferating tumors with nominal values of the parameters. $d_M = 3$ Gy, dashed lines; $d_M = 7$ Gy, solid lines.

aspects of the behaviour with n of $J^\star(n)$ and of the related quantities $g_e(n, d_n^\star)$, $g_l(n, d_n^\star)$, as depicted in Fig. 2. For comparison, the level of the cost function corresponding to the reference protocol is also reported. We notice that for any n at least one constraint in D_n is active, so that either the solution produces the maximal tolerable damage to at least one normal tissue or it equals $\tilde{d}$. Apart from changes in the trend of the cost function owing to weekend breaks (negligible in this context), changes in the slope of $J^\star(n)$ occur at values of n where the solution switches from one constraint boundary to another. Finally, changes in the trend of $J^\star(n)$ are determined by the onset of the accelerated repopulation occurring at kick-off time, either of the early normal tissue ($T_{Ke} = 7$ days, $n = 6$) and of the tumour ($T_K = 21$ days, $n = 16$).

If the tumour parameters are changed one at a time around the nominal value, the standard reference protocol keeps its optimality for rather broad variations of the parameters. As detailed in the following of this section, we verified, in agreement with previous results, that the sensitivity of the optimal fraction number to variations of T_K (spanning the estimated range $7 \div 28$ days) is rather low, except for low values of α and T_P (Yang and Xing, 2005; Saberian et al., 2015). On the contrary, the sensitivity of the optimal solution to variations of α (for ρ fixed) and of T_P is high, especially for negative variations with respect to the nominal value. Indeed, as it is evident from the expression (76) of the log cell kill, a reduction of α or T_P makes the repopulation term steeper, thus decreasing the value of n° and increasing the gain achievable in terms of LCK with respect to the standard protocol. We notice that LCK, and then $J^\star(n)$, actually depend on the

product αT_P.

Numerical examples to analyze in detail how the optimum changes when α, T_P, and ρ are supposed to change around the nominal value are illustrated in Tables 6a, 6b where, for each given pair α, T_P, the columns report the results for $\rho = 10$ Gy (left value) and $\rho = 50$ Gy (right value). When a single value is reported, the same optimum is obtained for any ρ ranging from 10 to 50 Gy (with 1 Gy steps). Also, the values of LCK and per cent LCK gain, defined as the relative LCK with respect to the reference protocol LCK, of the optimal solutions are reported. In these examples, we separately fixed α and ρ, for which more consistent estimates are available, while β is evaluated as $\beta = \alpha/\rho$.

Table 6a depicts the results for $T_K = 21$ days, while Table 6b reports the results for $T_K = 7$ days. Both tables have been obtained setting $d_M = 7$ Gy. In broad outline, Table 6a reveals that the results are substantially grouped in "blocks" corresponding to three types of optimal protocols: i) shorter than the reference and made of about 16 (or anyway less than 20) fractions of 3.1 Gy (or smaller) per fraction; ii) 35 fractions of 2 Gy, i.e. the reference protocol; iii) protracted protocols made of 40 fractions or more (up to 80) with size 1.8 Gy or less (up to 1.1 Gy).

So, an accelerated schedule of the kind 16F×3.1Gy proves to be optimal when a very fast tumour repopulation (short T_P) is accompanied by a rather low tumour intrinsic radiosensitivity α, clearly resulting in the most critical situation for the treatment outcome. Interestingly, for group i), it is $n^\circ = 16$ and $T(n^\circ) = 21$ days, so that the optimal treatment time equals the tumour kick-off time T_K.

Therefore, we can associate the inverse of the product αT_P to a tumour "aggressiveness scale" and we see that the optimality of the standard reference protocol is confirmed for intermediate values of αT_P. Large values of αT_P require instead to adopt longer protocols covering the quite wide range 40÷80 fractions, with dose per fraction of moderate intensity (1.8÷1.1 Gy). However, it can be noticed that the latter group of optimal schedules (type iii), though scattered, results in relatively concentrated LCK values, which are not too different from the reference LCK and reach a 7.9% gain only for the barely practicable case of 80 fractions, indicating as a possible sub-optimal strategy a standard treatment of this tumour class. By contrast, the short optimal schedule group can give remarkably high gains in terms of LCK with respect to the standard protocol (up to 123%). We note that for the smallest values of αT_P adopted in our simulations the reported LCK gain is infinite. Actually, in this case the standard reference protocol gives LCK ≤ 0 since, according to the LQ model, the tumour repopulation term overcomes the radiation damage term in expression (76), paradoxically implying that the therapy favours the tumour regrowth.

A similar pattern of the optimal number of fractions n° is obtained by changing the value of T_K, for instance setting $T_K = 7$ days (see Table 6b), as well as $T_K = 14$ or 28 days (results not shown). Clearly, for the same αT_P, the gain achievable in terms of tumour cell kill increases as the difference $|\bar{T} - T(n^\circ)|$ is increased and, as shown by Table 6b, it can exceed 600% for $T_K = 7$ days in protocols of type i).

It is important to remark that changing the fraction upper bound does not affect the solutions as long as d_M is greater than the largest optimal dose per fraction, which is equal to 3.1 Gy in Table 6a and 5.7 Gy in Table 6b. Indeed, if $d_M = 5$ Gy, for instance, Table 6a remains unchanged, while in 6b, being the solution 6F×5.7 Gy not admissible, the optimum would become 7F×5 Gy or 8F×4.7 Gy with LCK gains that can exceed 600%. Generally, as d_M decreases, the optimal protocol becomes longer with smaller LCK gains.

Similar results on the relationship between optimal treatment time and kick-off time have

Table 6: Sensitivity of the optimal solution d° to variations of T_P and α for $\rho \in [10, 50]$ Gy and $d_M = 7$ Gy. (a) $T_K = 21$ days; (b) $T_K = 7$ days. Bold values denote cases in which the "strong standard" protocol is optimal.

(a)

	$\alpha = 0.2$ Gy^{-1}				$\alpha = 0.35$ Gy^{-1}				$\alpha = 0.5$ Gy^{-1}			
T_P (days)	n°	Fraction size (Gy)	LCK	Gain (%)	n°	Fraction size (Gy)	LCK	Gain (%)	n°	Fraction size (Gy)	LCK	Gain (%)
1	16	3.1	5.6–4.5	∞	16	3.1	9.8–7.9	86.1–123.8	16	3.1	13.9–11.3	30.1–36.7
2	16	3.1	5.6–4.5	57.8–76.9	16–17	3.1–3	9.8–7.9	8.4–8.5	**35**	**2**	**14.5–12**	**0**
3	16	3.1	5.6–4.5	16.5–18.7	**35**	**2**	**10.3–8.6**	**0**	**35**	**2**	**15.7–13.3**	**0**
4	16–20	3.1–2.7	5.6–4.6	3–2.8	**35**	**2**	**10.9–9.2**	**0**	35–40	2–1.8	16.4–13.9	0–0.1
5	**35**	**2**	**5.8–4.8**	**0**	**35**	**2**	**11.3–9.6**	**0**	35–50	2–1.5	16.7–14.5	0–1.2
6	**35**	**2**	**6–5.1**	**0**	35–40	2–1.8	11.5–9.8	0–0.3	45–55	1.7–1.4	17–15.1	0.3–2.9
7	**35**	**2**	**6.2–5.2**	**0**	35–45	2–1.7	11.7–10.1	0–1.1	50–65	1.5–1.3	17.3–15.4	1–4.5
8	**35**	**2**	**6.4–5.4**	**0**	40–55	1.8–1.4	11.8–10.3	0.2–2.2	55–70	1.4–1.2	17.6–15.8	1.7–6.1
9	**35**	**2**	**6.5–5.5**	**0**	45–60	1.7–1.3	12–10.6	0.5–3.3	60–80	1.3–1.1	17.8–15.6	2.5–7.9

(b)

	$\alpha = 0.2$ Gy^{-1}				$\alpha = 0.35$ Gy^{-1}				$\alpha = 0.5$ Gy^{-1}			
T_P (days)	n°	Fraction size (Gy)	LCK	Gain (%)	n°	Fraction size (Gy)	LCK	Gain (%)	n°	Fraction size (Gy)	LCK	Gain (%)
1	6	5.7	4.6–3.3	∞	6	5.7	8.1–5.7	685.2–∞	6–8	5.7–4.7	11.5–8.3	77.4–102.9
2	6	5.7	4.6–3.3	223.5–623.6	6–10	5.7–4	8.1–6	17–15.3	**35**	**2**	**12.4–9.9**	**0**
3	6–10	5.7–4	4.6–3.4	36.4–39.7	**35**	**2**	**8.9–7.2**	**0**	**35**	**2**	**14.3–11.9**	**0**
4	6–15	5.7–3.1	4.6–3.5	5.8–3.8	**35**	**2**	**9.8–8.1**	**0**	35–40	2–1.8	15.3–12.9	0–0.1
5	**35**	**2**	**4.9–4**	**0**	**35**	**2**	**10.4–8.7**	**0**	35–50	2–1.5	15.9–13.6	0–1.3
6	**35**	**2**	**5.3–4.4**	**0**	35–40	2–1.8	10.8–9.1	0–0.3	45–55	1.7–1.4	16.3–14.3	0.4–3
7	**35**	**2**	**5.6–4.6**	**0**	35–45	2–1.7	11.1–9.5	0–1.2	50–65	1.5–1.3	16.7–14.8	1–4.7
8	**35**	**2**	**5.8–4.9**	**0**	40–55	1.8–1.4	11.3–9.8	0.2–2.3	55–70	1.4–1.2	17.1–15.2	1.8–6.3
9	**35**	**2**	**6–5**	**0**	45–60	1.7–1.3	11.5–10.1	0.6–3.5	60–70	1.3–1.2	17.4–15.6	2.6–7.7

been reported by Yang and Xing (2005); Fowler (2012). As pointed out by Fowler (1989, 2012), accelerated radiation therapy may be convenient for doubling times shorter than 2-3 days. The author also observed that only a minority of tumours would be expected to proliferate as fast as that, unless proliferation becomes even faster during the treatment than it was measured, for instance by flow cytometry, before the treatment starts. Indeed, the doubling time in a tissue

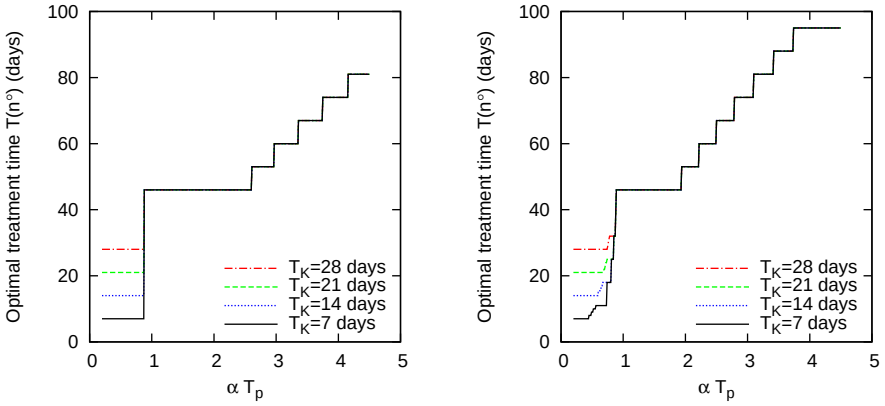

Figure 3: Optimal treatment time $T(n^\circ)$ as a function of αT_P for $\rho = 10$ Gy (left panel) and for $\rho = 50$ Gy (right panel). Daily dose upper bound $d_M = 7$ Gy.

during radiotherapy, T_P, is probably somewhat shorter than the pre-treatment potential doubling time, because a surviving fraction of previously resistant non-proliferating cells can return to cycle and rapidly repopulate, as a consequence of the reoxygenation following the irradiation (Bertuzzi et al., 2008, 2010).

A more complete and concise description of the results of this section is given by Figure 3, where it is shown how the optimal treatment time changes with the product αT_P, for $\rho = 10$, 50 Gy, $T_K = 7$, 14, 21, 28 days, and $d_M = 7$ Gy.

4.2. Slowly proliferating tumours

The most slowly proliferating tumours that are currently known are prostatic cancers, which, containing very low proportions of cycling cells (Brenner and Hall, 1999), exhibit long potential doubling times and low radiosensitivity ratios, the latter typically lower than the surrounding late-responding normal tissues identified by $\rho_l = 3$ Gy. For prostate tumours, Brenner and Hall (1999) estimated $\rho = 1.5$ Gy, with 95% confidence interval equal to $[0.8, 2.2]$ Gy, and $\alpha = 0.036$ Gy^{-1} (CI 95% $[0.026, 0.045]$). After Brenner and Hall (1999), many authors and major analyses agree in finding average α/β ratios smaller than 2 Gy, also reporting that ρ does not vary significantly with the tumour risk factors (Fowler, 2001; Fowler et al., 2003b; Gao et al., 2010; Proust-Lima et al., 2011; Miralbell et al., 2012; Dasu and Toma-Dasu, 2012; Fowler et al., 2013). However, other authors report higher estimates of α, $0.1 \div 0.15$ Gy^{-1} (see e.g. Wang et al. (2003); Yang and Xing (2005)) and some evidences of prostate cancers with higher radiosensitivity ratios falling in the range (ρ_l, ρ_e) can be found in the literature, as we will see in the next section.

Concerning the estimation of the tumour repopulation rate, an average *potential* doubling time (i.e. before any cell loss was induced by the treatment) of 40 days, with variability range between 9 and 60 days, was measured by Fowler et al. (2003b). However, the doubling time

during radiotherapy, T_P, is likely to be shorter than the potential doubling time because of the repoulation of radiation resistant non-cycling cells. In fact, Gao et al. (2010) report estimates of the doubling time, obtained by best fitting of clinical literature data, which are shorter and varying from 6 to 39 days. In the same study, the lag time T_K was estimated in the range $[27, 49]$ days. Other studies assume much longer kick-off times, up to 300 days (Yang and Xing, 2005).

On the basis of these results, we assume as nominal parameter values for the simulations $\rho = 1.5$ Gy, $\alpha = 0.1$ Gy^{-1}, $T_P = 28$ days, $T_K = 35$ days.

As shown by Tables 5a–5c, for tumours with low radiosensitivity ratios ($\rho < \rho_l$) the optimal solution tends to be hypofractionated, i.e. composed by few fractions of large size, and it would be made by a single fraction if d_M could exceed $\min\{\bar{A}_e(1,0), A_l(1,0)\}$. Hence, the choice of the limit d_M is expected to strongly affect the optimal schedule, and if d_M is allowed to increase, higher tumour cell kill and lower normal tissue BED compared to conventional regimes can be achieved by means of hypofractionated regimes.

One of the most consolidated protocols in prostate cancer treatment is the already mentioned "strong standard" protocol that we therefore keep as the reference for the computation of the tolerable $\text{BED}_l = 116.7$ Gy and $\text{BED}_e = 53.1$ Gy, as well as to perform the comparison among optimal schedules isoeffective with respect to the normal tissue complications. However, on the basis of our analytical results, hypofractionated schedules, like some schedules actually adopted in the clinical treatment of prostate cancer, are expected to be more "competitive" than the standard reference protocol.

The results of numerical simulations for the nominal parameter values are shown in Table 7, where d_M takes the values 2, 3, 5, 6, 7 Gy. When d_M increases, the optimal protocol consists in delivering a smaller total dose in a lower number of fractions, providing increased log cell kill, as well as higher LCK gain with respect to the standard 2 Gy protocol (up to 23%). We remark that in all the optimal protocols, the optimal number of non-zero fractions, in the following denoted by ν°, is smaller than n°, so that the optimal treatment time $T(n^\circ)$ is longer than the time strictly necessary to deliver the non-zero dose fractions only. We observe that this kind of solutions comes from the trade-off between shortening the treatment and keeping the daily dose fraction within the admissibility constraints. Indeed, protracting the treatment enables the early normal tissue to repopulate, which makes $k_e(n)$ larger, allowing comparatively larger fraction sizes.

Table 7: Optimal protocols for the nominal parameter set $\rho = 1.5$ Gy, $\alpha = 0.1$ Gy^{-1}, $T_P = 28$ days, $T_K = 35$ days, and for different upper bounds d_M. Reference protocol: $35\,\text{F} \times 2\,\text{Gy} = 70\,\text{Gy}/46$ days Fowler et al. (2003b).

d_M (Gy)	n°	$T(n^\circ)$ (days)	ν°	d°	Total dose (Gy)	LCK	Gain (%)
2	35	46	35	35F × 2 Gy	70	7.0	0
3	27	36	20	19F × 3 Gy + 1.69 Gy	58.69	7.57	8.56
5	19	24	9	8F × 5 Gy + 4.18 Gy	44.18	8.21	17.77
6	16	21	7	6F × 6 Gy + 3.82 Gy	39.82	8.40	20.49
7	13	16	5	5F × 7 Gy	35	8.61	23.49

It is interesting to compare the optimal solutions of Table 7 to real clinical protocols which, as seen before, suggested us plausible values of d_M. Table 8 summarizes the characteristics of these protocols, with $\hat{\nu}$ and $\hat{d}$ denoting number and size of the non-zero fraction doses, respectively, and $\hat{T}$ equal to the overall treatment length. From the comparison between Tables 7 and 8,

Table 8: Examples of hypofractionated clinical schedules for prostate cancer radiotherapy. $\hat{\nu}$, $\hat{d}$ are the number and size of non-zero fraction doses; $\hat{T}$ is the overall treatment time; F/w is the number of fractions delivered per week; BED_l, BED_e are computed as M_l/α_l, M_e/α_e according to (65), (64) with the fixed normal tissue parameters.

Protocol	$\hat{\nu}$	$\hat{d}$ **(Gy)**	**F/w**	**Total dose (Gy)**	$\hat{T}$ **(days)**	BED_l **(Gy)**	BED_e **(Gy)**	**Reference**
Princess Margaret	20	3	5	60	25	120	63.74	Martin et al. (2007)
Gunma Univ.	23	3	3	69	50	138	55.64	Akimoto et al. (2004)
Montreal Hosp.	9	5	1	45	56	120	28.68	Menkarios et al. (2011)
St. Thomas Hosp.	6	6	2	36	15	108	51.26	Collins et al. (1991)
Toronto Univ.	5	7	1	35	28	116.7	42.86	Tang et al. (2008)

it emerges that the optimal solution obtained for $d_M = \hat{d}$ is very similar to the real schedule adopting the same dose $\hat{d}$, particularly with respect to the number of fractions actually delivered ($\nu^\circ \simeq \hat{\nu}$). Small differences between these numbers (e.g. $\nu^\circ = 7$ vs. $\hat{\nu} = 6$ of St. Thomas protocol for $d_M = \hat{d} = 6$ Gy) can be attributed to the difference between the tolerable BED_e, BED_l that we have fixed, and those computed for the clinical schedules. Another example is given by the Gunma protocol for $\hat{d} = 3$ Gy that contains 23 fractions, but allows a larger BED_l compared to both Princess Margaret protocol and our optimal solution ($\nu^\circ = \hat{\nu} = 20$ with $d_M = \hat{d} = 3$ Gy). By contrast, not so small differences, and not always with the same sign, can be observed between the optimized and real treatment times, although the overall protocol patterns look similar since additional weekday breaks are envisaged (except for "Princess Margaret" protocol), that is $\hat{T} > T(\hat{\nu})$. Looking for example at the 5F×7 Gy protocol (Toronto University), which has $\text{BED}_l = 116.7$ equal to that reached by our optimal solution, we observe that the optimal protocol is shorter, as it includes less null dose fractions. Increasing n° by adding zero fractions, i.e. increasing $T(n^\circ)$ from 16 to 28 days, would actually give a sequence of optimal solutions all equivalent with respect to $J^\star(n)$ (no repopulation until $T_K = 35$ days) and producing the maximal late damage, M_l, but producing reduced early damages diverging from the permitted limit M_e.

We now investigate how the optimum obtained for a given d_M changes if the tumour parameters deviate from the nominal values. In the next simulations, starting from the nominal parameters, we compute the optimal protocols combining the following couples of parameter values: $\rho = 1.5 \pm 0.7$ Gy, $\alpha = 0.1 \pm 0.05$ Gy^{-1}, $T_P = 28 \pm 14$ days, $T_K = 35 \pm 7$ days. We assume ρ and α as independent parameters, so that β is computed as α/ρ. In Tables 9, 10 we report the results obtained for both $\rho = 0.8$ Gy and $\rho = 2.2$ Gy, and different combinations of the other parameters. Estimates of T_P and T_K taken from the literature indicate that rapid proliferation is usually associated to early repopulation onset (Gao et al., 2010), so that Tables 9, 10 refer to the pairs of the extreme values of $T_P = 14$ days, $T_K = 28$ days and $T_P = 42$ days, $T_K = 42$ days. First of all, we recognize that for the triples α, T_P, T_K assumed in these calculations, we get identical solutions either for $\rho = 0.8$ Gy and $\rho = 2.2$ Gy, as well as we verified to happen for any intermediate ρ in this range, even though the optimal LCK decreases continuously when ρ increases. On the whole, the optimal solutions are only slightly different from those of Table 7 and the only variation occurs for $d_M = 3$ Gy in $T(n^\circ)$ that passes from 36 days (Table 9, $T_K = 28$ days) to 37 days (Table 10, $T_K = 42$ days). We mention (without reporting the results) that, apart from a different value of LCK, optimal solutions identical to those of Table 9 are

obtained keeping $T_K = 28$ days but setting $T_P = 42$ days, while the results of Table 10 remain identical for $T_P = 14$ days, $T_K = 42$ days. To further analyse how variations of the tumour parameters around their nominal values possibly affect the optimal solutions, we searched the optimum for a sequence of problems with tumour parameters varying in the ranges $\rho \in [0.8, 2.2]$ Gy, $T_K \in [10, 100]$ days and, still supposing $alpha \in [0.05, 0.15]$ Gy^{-1}, we let αT_P vary in the interval $[0.05, 10]$ days/Gy. Figure 4 shows in fact the optimal solution as a function of αT_P for $d_M = 3$ Gy. We recall that in this section all the optima take the form $d_l(1, u)$ or $d_e(1, u)$, with u dependent on d_M and such that $u + 1 = \nu^\circ \leq n^\circ$ (see Tables 5a–5c). So, to identify an optimal protocol we have to specify not only n° (or $T(n^\circ)$), but also ν° and the size of the only fraction possibly different from d_M (residual fraction). For $d_M = 3$ Gy, the behaviours of these quantities at the optimum, reported in Fig. 4 for different T_K and for the extreme values of ρ, show a low sensitivity of the solution to parameter variations. Actually, appreciable variations with respect to the nominal solution of Table 7 can be noticed only for $\alpha T_P < 0.5$ days/Gy, or namely for $T_P < 0.5/\alpha \leq 10$ days which, according to the literature, represents an atypically short prostatic tumour doubling time. For $\alpha T_P > 0.5$ days/Gy, the number of radiotherapy sessions and the dose sizes do not change, while a one-day gap in $T(n^\circ)$ between 36 and 37 days can be noticed. This fact can be explained observing that if the tumour repopulation were absent, namely if $T_K \to \infty$, we would get $T(n^\circ) = 37$ days. Hence, as long as $T_K \geq 37$ days, the same optimum overall time is expected since no repopulation takes place for $n \leq n^\circ$. For $T_K < 37$ days, the optimal time $T(n^\circ)$ tends to become shorter (and mostly equal to 36 days) because in $J^\star(n)$ the increasing repopulation term contrasts the descent of the dose-dependent terms. For very small αT_P values, when the repopulation effect is remarkable, $T(n^\circ)$ tends to equal T_K. The patterns of the optimal quantities looks fairly similar for any chosen value of ρ, except for an increase in the threshold value of αT_P below which, when αT_P decreases, $T(n^\circ)$ shortens tending to T_K, while ν° reduces and the optimal residual dose fraction varies with respect to the "nominal" value 1.69 Gy.

For $d_M = 7$ Gy, a similar behaviour of the optimal solution is observed, as shown in Fig. 5. Here, for $T_K \to \infty$ the optimal treatment time would become $T(n^\circ) = 16$ days, which is therefore the same optimal value obtained for any $T_K \geq 16$ days. The behaviour of $T(n^\circ)$ with respect to αT_P and T_K, already observed for $d_M = 3$ Gy, can still be noted, including the one-day gap occurring between 15 and 16 days in this case. Moreover, the values of αT_P below which $T(n^\circ)$ approximates T_K are too small to be realistic for slowly proliferating tumours (less than 0.12 days/Gy for $\rho = 0.8$ Gy and less than 0.3 days/Gy for $\rho = 2.2$ Gy). On the contrary, the values of αT_P at which $T(n^\circ)$ switches from 15 to 16 days fall within the meaningful range of αT_P, i.e.

Table 9: Optimal protocols for $T_P = 14$ days, $T_K = 28$ days, $\alpha = 0.05, 0.15$ Gy^{-1}, $\rho = 0.8, 2.2$ Gy, and for different d_M values.

			$\alpha = 0.05$ Gy^{-1}		**$\alpha = 0.15$** Gy^{-1}	
d_M (Gy)	**$T(n^\circ)$ (days)**	**d°**	**LCK**	**Gain (%)**	**LCK**	**Gain (%)**
3	36	19F × 3 Gy + 1.69 Gy	5.8–2.8	18.0–12.1	17.8–8.8	14.4–5.8
5	24	8F × 5 Gy + 4.18 Gy	6.9–3.1	39.1–23.5	20.6–9.3	32.2–12.0
6	21	6F × 6 Gy + 3.82 Gy	7.1–3.1	44.4–24.9	21.4–9.4	37.2–13.2
7	16	5F × 7 Gy	7.4–3.2	50.2–26.4	22.2–9.5	42.7–14.6

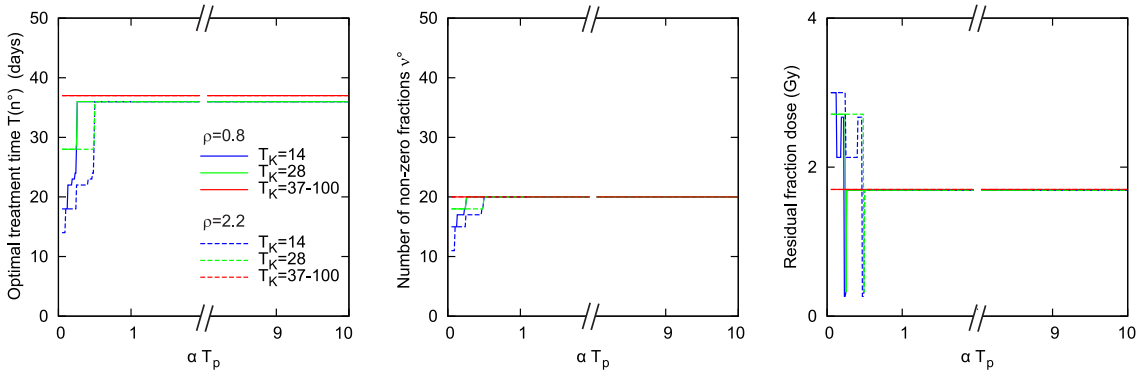

Figure 4: Sensitivity of the optimal protocol for slowly proliferating tumours to variations of αT_P, ρ and T_K. Daily dose upper bound $d_M = 3$ Gy.

1.58 days/Gy for $\rho = 0.8$ Gy and 3.96 days/Gy for $\rho = 2.2$ Gy. Also, it can be noticed that the optimal number of non-zero fraction doses does not change at all in these simulations ($\nu^\circ \equiv 5$). A behavior of the optimal quantities analogous to that reported for $d_M = 3$ and 7 Gy can be expected for intermediate values of the dose upper bound.

In view of the great uncertainty affecting the tumour parameter estimates, the fact that, for given values of the parameters related to normal tissues and d_M, the optimal solution is substantially insensitive to the tumour parameter changes appears to be a very favourable feature of the problem we are dealing with. Indeed, from a modelling point of view, the problem becomes that of providing a sufficiently accurate description of the healthy tissue constraints, along with reliable maximal damage bounds and a dose upper bound d_M.

For the case of two quadratic normal tissue constraints considered in the present study, the obtained results suggest the possibility of adopting, for each given d_M, a unique radiotherapy protocol for the treatment of tumours described by parameter values included among those assumed in this section. We propose to adopt, for each d_M, the possibly sub-obtimal solution holding in the largest interval of tumour parameter values. In particular, we can resolve the one-day uncertainty in the value of $T(n^\circ)$ choosing the largest value, which is always admissible. Moreover, we can disregard the changes of the solutions observed for small αT_P, obtaining the nominal solution of Table 7 (except for $d_M = 3$ Gy where we substitute $T(n^\circ) = 37$ days). The chosen solution,

Table 10: Optimal protocols for $T_P = 42$ days, $T_K = 42$ days, $\alpha = 0.05, 0.15$ Gy^{-1}, $\rho = 0.8, 2.2$ Gy, and for different d_M values.

			$\boldsymbol{\alpha = 0.05}$ Gy^{-1}		$\boldsymbol{\alpha = 0.15}$ Gy^{-1}	
$\boldsymbol{d_M}$ **(Gy)**	$\boldsymbol{T(n^\circ)}$ **(days)**	$\boldsymbol{d^\circ}$	**LCK**	**Gain (%)**	**LCK**	**Gain (%)**
3	37	19F × 3 Gy + 1.70 Gy	6.0–3.0	13.3–4.1	18.0–9.0	12.9–3.4
5	24	8F × 5 Gy + 4.18 Gy	6.9–3.1	29.7–8.1	20.6–9.3	29.2–7.4
6	21	6F × 6 Gy + 3.82 Gy	7.1–3.1	34.6–9.3	21.4–9.4	34.1–8.6
7	16	5F × 7 Gy	7.4–3.2	40.0–10.6	22.2–9.5	39.5–9.9

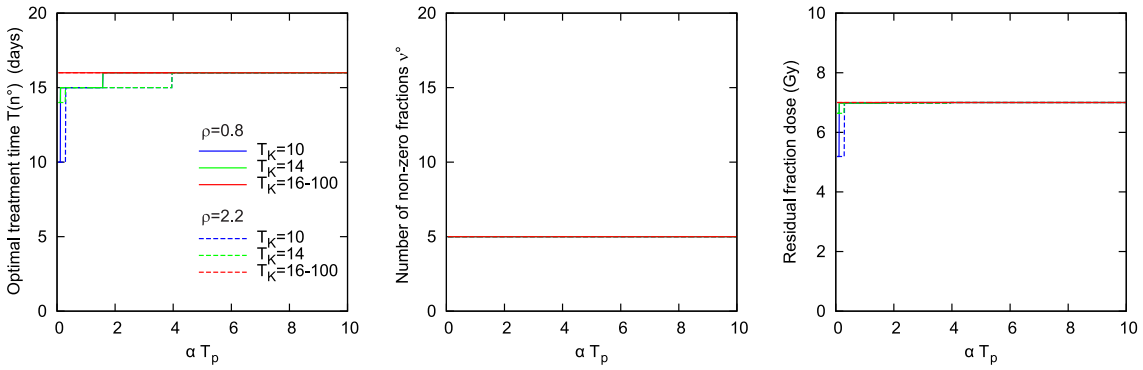

Figure 5: Sensitivity of the optimal protocol for slowly proliferating tumours to variations of αT_P, ρ and T_K. Daily dose upper bound $d_M = 7$ Gy.

beyond being robust, is always a safe solution, as it can be verified that it is compatible with the normal tissue constraints.

However, once the optimal hypofractionated protocol is determined for a given d_M, the choice of the inter-fraction time intervals, i.e. how to distribute the ν° fractions different from zero over the whole treatment course $T(n^\circ)$, remains undetermined as any dose spacing is equivalent within our formulation. In fact, the LQ model with exponential repopulation term that we adopted to describe the tumour response does not include kinetic effects due to multiple sequential irradiations, such as the effects originated by the non instantaneous sublethal damage repair and the resensitization process (LQR model by Brenner et al. (1995)). The main reasons that led us to adopt a "basic" LQ model were keeping the analytical formulation of the optimization problem simple and reducing the number of unknown biological parameters of the model. However, previous results on radiotherapy optimization indicate that including a term representing the sublethal damage due to incomplete repair in the LQ model affects the optimal schemes only negligibly (Yang and Xing, 2005; Bertuzzi et al., 2013), since typical values of the repair time (< 2 hours) are small compared to a one day inter-fraction time (Fowler et al., 2003b). With regard to the resensitization process, which includes both redistribution and reoxygenation, Yang and Xing (2005) investigated the effect of changing the resensitization time in the range of $1 \div 3$ days, observing that the optimal fractional dose distribution and the inter-fraction intervals actually do not change with the resensitization time. The authors also report the result that the optimized hypofractionated protocols contain two or three fraction doses per week, with nonzero fractions almost equally spaced over the entire treatment time.

Concerning the comparison among radiation schemes that differ only in the time spacing of the nonzero fractions, let us consider the (equivalent) optimal solutions exemplified in Fig. 6, obtained with $d_M = 7$ Gy and for the nominal parameter values used above to represent tumours with $\rho < \rho_l$. Incidentally, we observe that the treatment time of these solutions cannot be compressed, as delivering the same dose fractions during a time shorter than $T(n^\circ) = 16$ days would result in the violation of the early constraint. We searched the literature for clinical studies exploring the patient-assessed tolerance of real hypofractionated regimens. Among all, we mention some very recent works in which advancements in radiation therapy for prostate cancer management, including dose escalation (Brower et al., 2016), moderate and extreme hypofractionation (Koontz

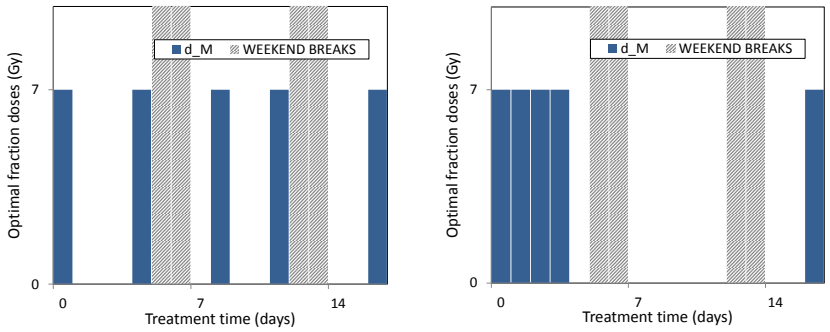

Figure 6: Two equivalent optimal protocols 5F×7 Gy with different dose spacing. Nominal values of tumour parameters and $d_M = 7$ Gy.

et al., 2015; Dulaney et al., 2016), are reviewed. In these papers, the efficacy, grade of toxicity, and quality of life outcomes of many hypofractionated protocols are evaluated and compared to standard fractionation schemes.

The comparison of our solutions with hypofractionated schedules used in prostate cancer treatment has to be restricted excluding, first of all, interstitial brachitherapy schemes and considering only examples of external-beam radiotherapy. So, we consider some IMRT applications of moderate (2.5-4 Gy per fraction) or extreme (5-10 Gy in 4-7 fractions) hypofractionation taken from the mentioned reviews. A further limitation, as reported by Koontz et al. (2015); Dulaney et al. (2016); Brower et al. (2016), concerns the prostate cancer stage, in that improved disease control has been obtained for low-risk and intermediate-risk stages only. High-risk prostate cancers, with high biological heterogeneity, appears to require combined approaches and therapy personalization (Dulaney et al., 2016; Dearnaley et al., 2016), so that our problem formulation might prove to be simplistic. Although short-term (rather than long-term) toxicity profiles are often available, summarizing the clinical data collected by the mentioned reviews, we see that only schemes with no more than two or three fractions per week, and almost uniformly spaced along the treatment time, have been considered and have produced acceptable toxicity rates. As an explicit example, King et al. (2012), for a 36.25 Gy/5F course of radiotherapy, observed a reduction of late urinary and late rectal toxicity for treatments with doses delivered three times a week on alternating days, versus consecutive daily treatments. So, diluted treatment schemes, like the one in the left panel of Fig. 6, appear to be preferable.

4.3. Tumours with intermediate radiosensitivity ratio

The behaviour of tumours characterized by values of ρ included between ρ_l and ρ_e may shift from fast (compared with late normal tissues) to slow (compared with early normal tissues). Therefore, the optimal radiotherapy strategy may noticeably vary depending on all the tumour parameters. The trade-off situation for $\rho_l \leq \rho < \rho_e$ is reflected in the different optimal structures provided by Tables 5a and 5c, as well as in the possible existence, for some n values, of an infinite set of equivalent optimal solutions formed by the points on the intersection of the early and late

constraint boundaries that satisfy the limit d_M.

The first example to illustrate the solution behaviour for the class of tumours with $\rho_l \leq \rho < \rho_e$ concerns breast cancer. Conventional schedules for whole-breast irradiation after breast-conserving surgery consist of 1.8 to 2 Gy daily fractions given 5 times a week to a total dose of 45 to 50 Gy over 5 weeks (Whelan et al., 2008). So, in the current example, we assume the reference values $\bar{n} = 25$, $\bar{d} = 1.8$ Gy, $\bar{T} = 32$ days for the computation of the maximal tolerable adverse effect on late and early normal tissues. Then, keeping the normal tissue parameters to the values used in all the numerical simulations, we have BED_l=72 Gy and BED_e=33.3 Gy.

Following the introduction and validation of the mentioned reference schedule, experimental evidences of a rather low radiosensitivity ratio for breast cancer, along with the technical advancements in radiotherapy, have drawn a growing interest for hypofractionated schedules in which a total dose approximately equal to that of the reference protocol (45 Gy) is delivered over a shorter time length (Yarnold et al., 2005; Whelan et al., 2008; Qi et al., 2011). Examples of such hypofractionated schedules consist of daily fractions ranging from 2 to 3.3 Gy delivered in 16 fractions over 22 days (three weeks), with an optional boost of 10-16 Gy in 1-1.5 weeks. As to the upper bound d_M, taking values of the fraction doses from the clinical literature, we set: $d_M = 2$, 2.25, 2.5, 3, 3.3 Gy.

Concerning the tumour parameters, the best estimate $\rho = 4$ Gy is reported by Whelan et al. (2008) and confirmed by Yarnold et al. (2005) and Qi et al. (2011), even though the coefficient of variation of the estimates can be as high as to give α/β close to $\rho_e = 10$ Gy or even falling below $\rho_l = 3$ Gy. We will consider for ρ the values 4 and 8 Gy. Qi et al. (2011) used the generalized LQ model to fit survival data from a series of randomized clinical trials, obtaining the estimates $\alpha = 0.08 \pm 0.02$ Gy^{-1} and $T_P = 14 \pm 7.8$ days. Hence, we assume the following nominal set of tumour parameters: $\rho = 4$ Gy, $\alpha = 0.12$ Gy^{-1}, $T_P = 14$ days, and $T_K = 28$ days (T_K is set to an intermediate value between the kick-off times of slowly and fast proliferating tumours in the absence of experimental indications).

Table 11: Optimal protocols for the nominal parameter set $\rho = 4$ Gy, $\alpha = 0.12$ Gy^{-1}, $T_P = 14$ days, $T_K = 28$ days, and for different values of d_M. Reference protocol: $25\,\text{F} \times 1.8\,\text{Gy} = 45\,\text{Gy}/32$ days (Whelan et al., 2008).

d_M (Gy)	n°	$T(n^\circ)$ (days)	ν°	d°	Total dose (Gy)	LCK	Gain (%)
1.8	25	32	25	25F × 1.8 Gy	45.4	3.31	0
2	24	31	23	22F × 1.94 Gy + 1.08 Gy	43.76	3.32	0.20
2.25	22	29	19	18F × 2.21 Gy + 1.91 Gy	41.69	3.33	0.61
≥ 2.5	21	28	18	17F × 2.36 Gy + 0.41 Gy	40.53	3.34	0.82

Table 11 shows the results obtained for the nominal values of breast cancer parameters and for different d_M values. In this example, the optimal solution is given by any of the vectors on the intersection between the late and early constraint boundaries, among which for each d_M we choose the representative vector d^R reported in Table 11.

We remind that, for each n, d^R is the n-dimensional vector with entry sum S (see Eq. (25)), and containing $[v]$ entries equal to $R_{1[v]}$ (Eq. (36)). In view of the dependence of v on n, $R_{1[v]}$ can be seen as a function of n, which is defined as long as $v \leq n$. We also note that in our setting, because of Eqs. (66) and (67), any reference protocol satisfies both the early and late constraint with the equality sign and it actually coincides with the vector d^R at $n = \bar{n}$. Fig. 7

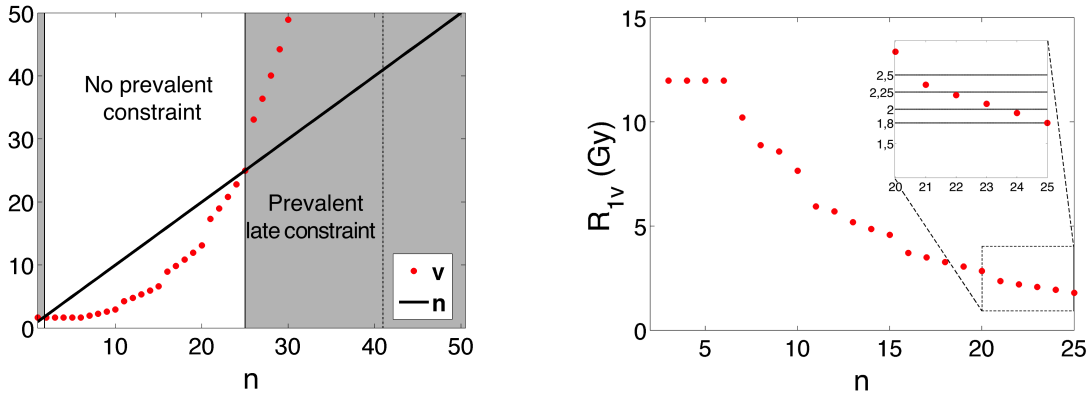

Figure 7: Profile of v for $n \in [1, 50]$ and $R_{1[v]}$ for $n \in [2, 25]$.

shows the plots of v (left panel) and $R_{1[v]}$ (right panel) in suitable intervals of n, computed using the reference protocol $25\,\mathrm{F} \times 1.8\,\mathrm{Gy} = 45\,\mathrm{Gy}/32$ days. It can be noted that $R_{1[v]}$ is defined for $v \leq n$, that is for $n \in [2, \bar{n}]$, with $\bar{n} = 25$ in Fig. 7.

Comparing the results of Table 11 and the pattern of $R_{1[v]}$ in Fig. 7, it can be observed that, as long as $d_M \leq 2.5$ Gy, the optimal solution for a certain d_M is given by the vector d^R having the largest entry $R_{1[v]}$ consistent with the constraint $R_{1[v]} \leq d_M$. This maximal value of $R_{1[v]}$ identifies on the $R_{1[v]}$ vs. n plot the value of n corresponding to n°, as shown by the box in the right panel of Fig. 7 where $R_{1[v]}$ is detailed for $n \in [20, 25]$. However, the optimal solution obtained for $d_M > 2.5$ Gy is the same obtained for $d_M = 2.5$ Gy. This can be explained by noting that if d_M is so large as to intercept the $R_{1[v]}$ plot for $n < n_K$, where $J^\star(n)$ is certainly non-increasing, then the optimal solution is always $n^\circ = n_K$, with $n_K = 21$ in our example. Looking at the LCK gains in Table 11, we also notice that very small gains (less than 1%) are obtained with respect to the reference protocol for any d_M, although increasing d_M has the advantage of permitting shorter treatment lengths and smaller total doses.

Because of the uncertainty affecting the parameter estimates, it is opportune to evaluate the sensitivity of the optimal nominal solutions to variations of the parameter values. Table 12 reports the optimal solutions for $\rho = 4$ Gy, $T_K = 28$ days, $d_M = 2.5$ Gy and for $\alpha = 0.1, 0.12, 0.14$ Gy^{-1} with T_P variable in $[7, 28]$ days with one day step. For these parameter values, we found that vectors on the intersection of the boundaries of the normal tissue constraints (represented by d^R) are optimal. Denoting by $d^R_{n^\circ}$ the vector d^R at $n = n^\circ$, only two optimal protocols are recognized in Table 12: d^R_{21} for small values of the product αT_P, and d^R_{25}, i.e. the reference protocol, for αT_P large.

To further investigate the solution behaviour when the tumour parameters vary, we simulated the optimum as a function of αT_P, for different values of T_K, for $\rho = 4$ Gy and setting $d_M = 2.5$ Gy. Figure 8 reports the values of n° obtained with αT_P ranging with 0.01 steps in $0.05 \div 10$ days/Gy. As the value of n° alone does not identify the entire optimal schedule, we need to supplement the results of Fig. 8 with the following comments. As expected, large variations of the parameter values can result in different types of optimal schedules. The first distinction concerns the kick-off time T_K since, as illustrated by Fig. 8, the optimal protocol depends on whether T_K is shorter (left panel) or longer (right panel) than $\bar{T}$. For $T_K \leq \bar{T}$ (left panel of Figure 8), similarly to Table 12, the optimum is of the kind d^R, with $n^\circ = 21$ or 25 for the

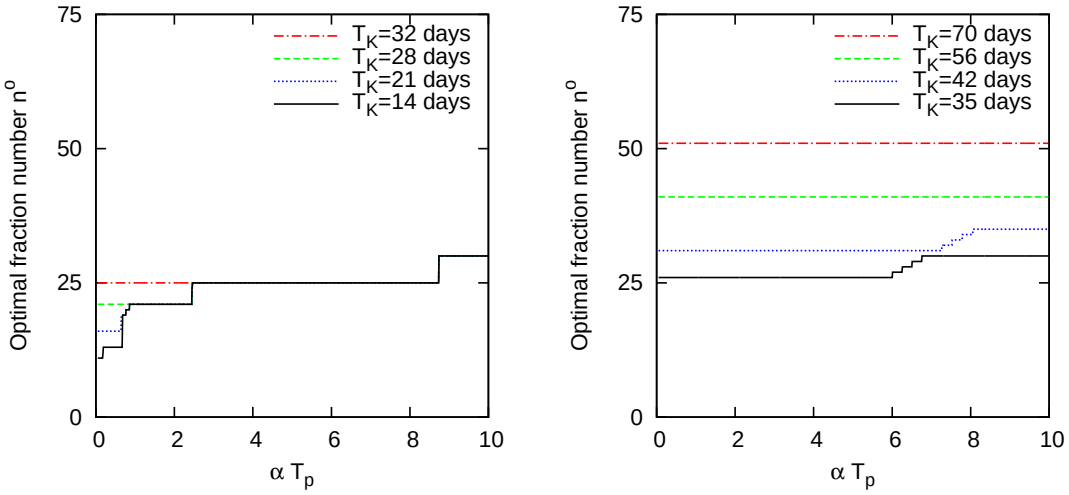

Figure 8: Sensitivity of the optimal protocol to variations of αT_P and T_K for $\rho = 4$ Gy. Left panel: $T_K \leq \bar{T}$; right panel: $T_K > \bar{T}$. Daily dose upper bound $d_M = 2.5$ Gy. Reference protocol: $25\,\mathrm{F} \times 1.8\,\mathrm{Gy} = 45\,\mathrm{Gy}/32$ days.

majority of αT_P values (from 0.86 to 8.73 days/Gy). For small αT_P, n° is smaller than $\bar{n}$ and the solution can be either $\tilde{d}$ or of the kind $d_e(1, u)$, depending on d_M. The solutions obtained for low αT_P, being rather different from the reference fractionation, can reach very high LCK gain with respect to the reference protocol. Such solutions are reported in Fig. 8 for completeness of the analysis, although the estimated values of α and T_P for tumours having $\rho_l \leq \rho < \rho_e$ indicate that the product αT_P is likely greater than about 0.4 day/Gy (Whelan et al., 2008). On the other hand, if αT_P is large, the solution becomes equi-fractionated and equal to $d_l(n^\circ, 0)$, with $n^\circ > \bar{n}$, providing only little gain with respect to the reference protocol (LCK gain $< 1\%$).

As depicted in the right panel of Fig. 8, when T_K is longer than $\bar{T}$, the optimal fractionation pattern is given by $d_l(n^\circ, 0)$, and the optimal fraction number n° turns out to be equal to n_K for almost all the considered αT_P interval, or slightly greater than n_K if accelerated repopulation is weak (αT_P not small). However, the achieved LCK gain is only about 3.2% at most, for $T_K = 70$ days and $\alpha T_P = 10$ days/Gy. Moreover, we notice that such prolonged optimal treatments, like for instance $T(n^\circ) = T_K = 70$ days, are not easily feasible in practice.

Table 12: Sensitivity of the optimal solution to variations of T_P and α for $\rho = 4$ Gy, $T_K = 28$ days, and $d_M = 2.5$ Gy. Optimal protocols: $25\,\mathrm{F} \times 1.8\,\mathrm{Gy} = 45\,\mathrm{Gy}/32$ days ($d_{21}^R \equiv$ Ref.); 17F $\times$ 2.36 Gy + 0.41 Gy = 40.53 Gy/28 days (d_{21}^R).

	$\alpha = 0.1$ Gy^{-1}			$\alpha = 0.12$ Gy^{-1}			$\alpha = 0.14$ Gy^{-1}		
T_P (days)	d°	LCK	Gain (%)	d°	LCK	Gain (%)	d°	LCK	Gain (%)
7–17	d_{21}^R	2.78	4.62–0.78	d_{21}^R	3.34	3.5–0.36	d_{21}^R	3.9	2.72–0.05
18–20	d_{21}^R	2.78	0.64–0.51	d_{21}^R	3.34	0.24–0.04	Ref.	3.9–3.91	0
21–24	d_{21}^R	2.78	0.3–0.04	Ref.	3.34–3.35	0	Ref.	3.91–3.92	0
25–28	Ref.	2.79	0	Ref.	3.35–3.36	0	Ref.	3.92	0

Taking the same variability range of αT_P and the same values of T_K, we investigated the behaviour of the optimal solution increasing the radiosensitivity ratio up to $\rho = 8$ Gy (results not shown). A behaviour similar to $\rho = 4$ Gy is obtained for this larger ρ, although the optimal solution becomes equi-fractionated with $n^\circ \geq \bar{n}$ for the majority of αT_P values (≥ 0.98 days/Gy). The longest of such solutions has $n^\circ = 65$ but the resulting LCK gain is lower than 5.5% for $T_K \leq \bar{T}$, and lower than 10.1% for $T_K > \bar{T}$.

Overall, the simulations for $\rho = 4$ Gy and $\rho = 8$ Gy assuming $d_M = 2.5$ Gy, show that for the majority of αT_P values, the optimal solutions are characterized by $n^\circ \geq \bar{n}$ and $d^\circ \leq \bar{d}$, so that they are not affected by a different choice of the daily upper bound. Moreover, as seen above, optimal solutions strictly longer than $\bar{n}$ do not provide significant advantage in terms of LCK. Therefore, as the knowledge about the actual parameter values is scarce, we deem it useful to treat breast tumours exploiting the reference fractionation usually adopted in clinical practice.

It is of note to consider, as a final numerical example for $\rho_l \leq \rho < \rho_e$, $\rho = 6$ Gy that can suitably represent prostatic cancers not assimilable to slowly proliferating tumours (Oliveira et al., 2012). In fact, since the work by Brenner and Hall (1999) who estimated an α/β ratio lower than that of late responding normal tissues, the value of the radiosensitivity ratio of prostatic cancer has been long debated. The paper by Oliveira et al. (2012) gives a comprehensive survey of the literature on this subject, reporting several estimates of α/β, obtained both from clinical and experimental data of prostate cancers, and discussing factors that potentially contribute to the uncertainty about the estimation of this value. Such factors include: heterogeneity of tumors, interpatient variations, clinical tumour stage, hypoxia, presence of clonogenic cells, effectiveness of external-beam radiotherapy, and measurement modality. Without going into the details of

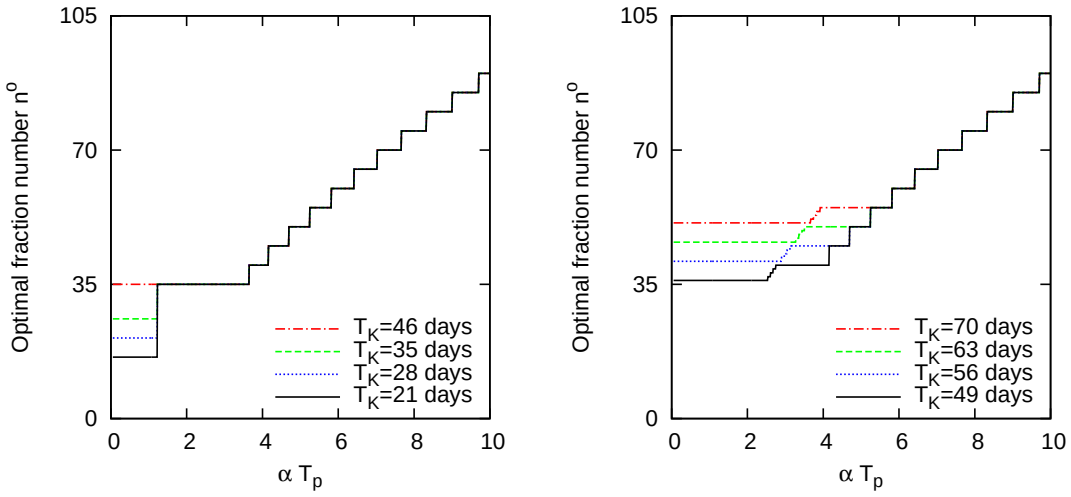

Figure 9: Sensitivity of the optimal protocol to variations of αT_P and T_K for $\rho = 6$ Gy. Left panel: $T_K \leq \bar{T}$; right panel: $T_K > \bar{T}$. Daily dose upper bound $d_M = 7$ Gy. Reference protocol: $35\,\mathrm{F} \times 2\,\mathrm{Gy} = 70\,\mathrm{Gy}/46$ days.

these evaluations (that can be found in the exhaustive bibliography of the paper by Oliveira et al. (2012)), we refer to some results reporting values of ρ in $[\rho_l, \rho_e)$, and precisely giving the average estimate $\rho = 6$ Gy, together with the estimate $\alpha = 0.1 \div 0.35$ Gy^{-1} (Nahum et al., 2003; Carlson et al., 2004). Moreover, Wang and Li (2005) have shown, by means of in situ measurements of

prostate cancer patients, that the potential doubling time of tumor cells has a large variation, ranging from 15 to 170 days. On the basis of these findings, we assume the following nominal parameter values for the prostate example: $\rho = 6$ Gy, $\alpha = 0.2$ Gy^{-1}, and $T_P = 14$ days, while T_K is set to 28 days, which is an intermediate value between the nominal values of slowly and fast proliferating tumours.

As for the reference protocol, we switch back to the "strong standard" protocol $35\,\mathrm{F} \times 2\,\mathrm{Gy} = 70\,\mathrm{Gy}/46$ days, commonly used for prostate cancer treatment. Setting the tumour parameters to the mentioned nominal values, we computed the optimal solutions for different values of d_M. The reference protocol proved to be optimal irrespective of d_M. Figure 9 reports the results of the numerical simulations assuming $\rho = 6$ Gy, $d_M = 7$ Gy, and different values of T_K ($T_K \leq \bar{T}$, left panel, and $T_K > \bar{T}$, right panel), with αT_P ranging in $0.05 \div 10$ days/Gy (step 0.01). Figure 9 shows that for the majority of αT_P values, the optimal solutions are characterized by $n^\circ \geq \bar{n}$ and $d^\circ \leq \bar{d}$. So, for $\rho = 6$ Gy, the tumour behaves like a fast proliferating tumour (similarly to the breast cancer example with $\rho = 8$ Gy). We note that $\rho = 6$ Gy was also assumed for prostate cancer cases in the theoretical paper by Saberian et al. (2015) concerning the fractionation optimization in radiotherapy. Although multiple normal tissue constraints are considered, the results obtained in that paper are comparable to ours, in that the tumour behaves like a fast proliferating tumour with respect to the (most restrictive) late responding tissue.

In summary, this numerical example again suggests to adopt the standard fractionation scheme since the optimal solutions strictly longer than $\bar{T}$ provide LCK gains not higher than 5.7%.

5. Concluding remarks

We addressed the problem of finding the optimal dose fractionation for cancer radiotherapy schedules of the kind one fraction/day, five fractions/week, representing the tumour and normal cell responses to radiation by means of the LQ model with exponential repopulation. The problem is formulated as a constrained nonlinear programming problem in terms of the vector of the dose sizes, d, and of the total number of dose fractions, n. Based on the chosen radiotherapy scheme, the total treatment duration is expressed in terms of the number of fractions by a fixed relationship and it is not an independent decision variable. Two types of healthy tissues, namely the early and late responding tissues are considered, and both linear and quadratic constraints are imposed to limit the adverse effects of the irradiation.

We proposed a procedure to solve the optimization problem in two consecutive steps: i) analytical determination of the optimal fractionation protocol, d_k, $k = 1, \ldots n$, as a function of the model parameters for a fixed, but arbitrary number of fractions n; ii) numerical computation for specific parameter settings of the optimal number of treatment sessions, and of the optimal treatment time, by means of a finite number of direct comparisons among the cost function values obtained for the sequence of the optima with n fixed, $n = 1, \ldots, n_M$.

The analytical study developed in part i) provides a framework to determine the optimal fractionation schedule over a given treatment length as a function of the tumour type and of the fraction upper bound, as well as of the normal tissue parameters. The generality of the approach at step i) relies on the representation of the tumour response by means of a cumulative LQ model with a set of four parameters. Such a simplified representation can be adopted in the external beam radiotherapy planning for the management of early-stage disease cases (Dearnaley et al., 2016). As a further assumption concerning the normal tissue constraints, we suppose that the maximal admissible levels of early and late complications, as well as the maximal size of the daily

dose d_M, are assigned. However, the study is developed without restrictions about the parameter values, in order to give the optimal solution in terms of general (positive) values of the model parameters.

Despite the simplified modelling assumptions, the analytical determination of the optimal solutions for n fixed proved to be rather complex. The results are in agreement with our previous works (Bertuzzi et al., 2013; Bruni et al., 2015) and the solutions hold for any value of n. Provided that d_M is not so restrictive as to make the early and late constraints unnecessary, a first property of the solutions is that, the optimal protocols produce the maximal tolerable damage to at least one normal tissue, with optimal fraction sizes dependent on the normal tissue parameters and on the daily upper bound, but independent on the tumour radiosensitivity ratio ρ. However, the value of ρ compared to the radiosensitivity ratio of normal tissues, influences the optimal scheme of dose fractionation. In particular, when d_M is sufficiently large, hypofractionated protocols are convenient for tumours with low ρ values, such as most prostatic cancers, whereas the uniform fractionation tends to be optimal for tumours with high ρ. As expected, even for small ρ, if the dose upper bound gets "stricter", the optimal protocol becomes more prolonged, and eventually uniform when d_M is very low. This result is consistent with the clinical and bio-mathematical literature (Fowler, 2010; Yang and Xing, 2005; Brenner and Hall, 1999; Fowler et al., 2003b) and confirms the results obtained by Bertuzzi et al. (2013) and by Bruni et al. (2015). Finally, we complete the analytical picture of the optima by showing the existence of a possibly infinite set of equivalent optimal schedules for tumours having radiosensitivity ratios intermediate between those of the early and late responding normal tissues.

In part ii) of the work, we performed the numerical simulations focusing on the three mentioned tumour classes characterized by radiosensitivity ratios belonging to the intervals $\rho \geq \rho_e$, $\rho < \rho_l$ and $\rho_l \leq \rho < \rho_e$. For all the classes considered, we fixed the normal tissue parameters according to the literature (Yang and Xing, 2005; Fowler, 2010) and we investigated how changes of the remaining tumour parameters, along with the value of the daily dose upper bound, affect the optimal solution.

To quantify the maximum admissible damages to the normal tissues, the quantities $k_e(n)$ and k_l are expressed by means of the Biologically Effective Dose (Barendsen, 1982; Yang and Xing, 2005; Fowler, 2010), so that these values become dependent on the model used to represent the damage and on a tolerable clinical protocol chosen as the reference protocol. However, this choice allowed us to establish some properties related to the geometric prevalence of the constraints for each optimization problem with n fixed. This fact implies that the geometry of all the optimization problems can be known "a priori", before performing the numerical comparisons. Furthermore, we were able to easily establish the boundedness of the optimal number of fractions for the tumour classes considered in the numerical simulation section. The optimization of the number of treatment sessions led to optimal schedules that confirm the results highlighted in the first part of the work concerning the influence of ρ on the fractionation scheme. Aim of the numerical simulation section was to provide the optimal solution investigating broad ranges of the parameter values, while providing a schematic summary of the results. It should however be stressed that the practical applicability of the obtained results is limited by the difficulty in assessing the model parameter values for highly heterogeneous populations such as the human tumours. Moreover, the role of the product αT_P in determining the optimal treatment length has been evidenced. The quantity αT_P can be seen as an inverse measure of the tumour aggressiveness, in that small values of this product are associated to very fast tumour repopulation accompanied by a rather low intrinsic radiosensitivity of the tumour.

Let us now discuss in further detail the main results obtained for the three classes of tumours. For tumours having $\rho \geq \rho_e$, such as the head and neck cancer, the reference "strong standard" protocol, $35\,\mathrm{F} \times 2\,\mathrm{Gy} = 70\,\mathrm{Gy}/46$ days, is optimal for the majority of the considered tumour parameter values. However, for the same tumour class, we also found that tumours characterized by low values of the product αT_P should be treated by accelerated schedules since the achievable LCK could be very high compared to the reference protocol.

For tumours having $\rho < \rho_l$ (e.g. prostate cancer), hypofractionated schedules are more "competitive" then the "strong standard" protocol, frequently used also for the treatment of prostate cancer. As shown by the numerical simulations, when the daily dose upper bound increases the optimal protocol consists in delivering a smaller total dose in a lower number of fractions, providing a higher LCK gain with respect to the standard 2 Gy protocol. Such solutions are generated by the trade-off between shortening the treatment and keeping the daily dose fraction within the admissibility constraints. We proposed a specific protocol for different values of the upper bound d_M and we verified that such protocols remain optimal for a wide range of the tumour parameters. The evidence that the optimal solution is substantially insensitive to the tumour parameter changes is a favourable feature as the tumour parameter values are characterized by high uncertainty. The proposed optimal solutions are always safe solutions, i.e. compatible with the normal tissue constraints, and they are similar to the hypofractionated protocols already used in the clinical treatment of prostate cancer. We also found that for very small αT_P values, when the repopulation effect is remarkable, the optimal treatment time $T(n^\circ)$ tends to be equal to the kick-off time T_K. However, the values of αT_P for which $T(n^\circ)$ approximates T_K are too small to likely represent slowly proliferating tumours.

For tumours having $\rho_l \leq \rho < \rho_e$, e.g. breast cancer or prostate cancer not assimilable to slowly proliferating tumours, either the structure and the length of optimal solutions strongly depend on the tumour parameters. The optimal solutions may result in different types of schedules, close to fast-like schedules or to slow-like schedules, depending on their radiosensitivity/proliferative behaviour which may shift from fast (compared with late normal tissues) to slow (compared with early normal tissues). However, for the tumour types considered and for the majority of the related tumour parameters, we obtained equi-fractionated optimal solutions, which are either equal to or longer than the reference protocol. Moreover, as the optimal solutions longer than the standard treatment do not provide significant advantage in terms of LCK, we suggest to treat both the considered tumours by means of the related standard scheme of fractionation actually used in clinical practice. Also for these examples, low values of αT_P provide short schedules rather different from the reference fractionation. As noted for slowly proliferating tumours, such solutions, despite high LCK gains with respect to the reference protocol, can be neglected since the estimated values of α and T_P found in the literature indicate higher values of the product αT_P.

We finally remark that for most of αT_P values two have been found to be optimal: the standard 2 Gy protocol for $\rho \geq \rho_l$ and the hypofractionated protocols for $\rho < \rho_l$, provided that large doses may safely delivered. When experimental or clinical evidences indicate very low αT_P values, different (shorter) protocols may be optimal.

Acknowledgments The authors gratefully thank Dr. Alessandro Bertuzzi for clarifying discussions and helpful suggestions. FP is supported by SysBioNet, Italian Roadmap Research Infrastructures 2012. FC is supported by The Epigenomics Flagship Project (Progetto Bandiera Epigenomica), EPIGEN, funded by the Italian Ministry of Education, University and Research (MIUR), and the National Research Council (CNR).

References

T. Akimoto, H. Muramatsu, M. Takahashi, J. Saito, Y. Kitamoto, K. Harashima, Y. Miyazawa, M. Yamada, K. Ito, K. Kurokawa, H. Yamanaka, T. Nakano, N. Mitsuhashi, and H. Niibe. Rectal bleeding after hypofractionated radiotherapy for prostate cancer: correlation between clinical and dosimetric parameters and the incidence of grade 2 or worse rectal bleeding. *Int. J. Radiat. Oncol. Biol. Phys.*, 60:1033–1039, 2004.

M. Astrahan. Some implications of linear-quadratic-linear radiation dose-response with regard to hypofractionation. *Med. Phys.*, 35:4161–4172, 2008.

H. Badri, K. Pitter, E.C. Holland, F. Michor, and K. Leder. Optimization of radiation dosing schedules for proneural glioblastoma. *J. Math. Biol.*, 72:1301–1336, 2016.

G. W. Barendsen. Dose fractionation, dose rate, and isoeffect relationships for normal tissue responses. *Int. J. Radiat. Oncol. Biol. Phys.*, 8:1981–1997, 1982.

A. Bertuzzi, A. Fasano, A. Gandolfi, and C. Sinisgalli. Reoxygenation and split-dose response to radiation in a tumour model with Krogh-type vascular geometry. *Bull. Math. Biol.*, 70: 992–1012, 2008.

A. Bertuzzi, C. Bruni, A. Fasano, A. Gandolfi, F. Papa, and C. Sinisgalli. Response of tumor spheroids to radiation: Modeling and parameter identification. *Bull. Math. Biol.*, 72:1069–1091, 2010.

A. Bertuzzi, C. Bruni, F. Papa, and C. Sinisgalli. Optimal solution for a cancer radiotherapy problem. *J. Math. Biol.*, 66:311–349, 2013.

T. Bortfeld, J. Ramakrishnan, J. N. Tsitsiklis, and J. Unkelbach. Optimization of radiation therapy fractionation schedules in the presence of tumor repopulation. *Med. Phys.*, pages 1–40, 2015.

D. J. Brenner. The linear-quadratric model is an appropriate methodology for determining isoeffective doses at large doses per fraction. *Semin. Radiat. Oncol.*, 18:234–239, 2008.

D. J. Brenner and E. J. Hall. Fractionation and protraction for radiotherapy of prostate carcinoma. *Int. J. Radiat. Oncol. Biol. Phys.*, 43:1095–1101, 1999.

D. J. Brenner, L. R. Hlatky, P. J. Hahnfeldt, E. J. Hall, and R. K. Sachs. A convenient extension of the linear-quadratic model to include redistribution and reoxygenation. *Int. J. Radiat. Oncol. Biol. Phys.*, 32:379–390, 1995.

J.V. Brower, J.D. Forman, P.A. Kupelian, D.G. Petereit, V. Gondi, C.A. Lawton, N. Anger, S. Saha, R. Chappell, and M.A. Ritter. Quality of life outcomes from a dose-per-fraction escalation trial of hypofractionation in prostate cancer. *Radiat. Oncol.*, 118:99–104, 2016.

C. Bruni, F. Conte, F. Papa, and C. Sinisgalli. Optimal weekly scheduling in fractionated radiotherapy: effect of an upper bound on the dose fraction size. *J. Math. Biol.*, 71:361–398, 2015.

D.J. Carlson, R.D. Stewart, X.A. Li, K. Jennings, J.Z. Wang, and M. Guerrero. Comparison of in vitro and in vivo α/β ratios for prostate cancer. *Physics in Medicine and Biology*, 49: 4477–4491, 2004.

C. D. Collins, R. W. Lloyd-Davies, and A. V. Swan. Radical external beam radiotherapy for localised carcinoma of the prostate using a hypofractionation technique. *Clin. Oncol. (R. Coll. Radiol.)*, 3:127–132, 1991.

F. Conte, F. Papa, and C. Sinisgalli. Minimum value of the maximal entry of n-dimensional vectors with constant sum of the entries and of the squared entries. *IASI-CNR Technical Report*, R.10:1–17, 2015.

A. Dasu and I. Toma-Dasu. Prostate alpha/beta revisited – an analysis of clinical results from 14168 patients. *Acta Oncol.*, 51:963–974, 2012.

D. Dearnaley, I. Syndikus, H. Mossop, V. Khoo, A. Birtle, D. Bloomfield, J. Graham, P. Kirkbride, J. Logue, Z. Malik, J. Money-Kyrle, J. M. O'Sullivan, M. Panades, C. Parker, H. Patterson, C. Scrase, J. Staffurth, A. Stockdale, J. Tremlett, M. Bidmead, H. Mayles, O. Naismith, C. South, A. Gao, C. Cruickshank, S. Hassan, J. Pugh, C. Griffin, E. Hall, and CHHiP Investigators. Conventional versus hypofractionated high-dose intensity-modulated radiotherapy for prostate cancer: 5-year outcomes of the randomised, non-inferiority, phase 3 chhip trial. *Lancet Oncol.*, 2016. doi:10.1016/S1470-2045(16) 30102-4.

D. D. Dionysiou, G. S. Stamatakos, N. K. Uzunoglu, K. S. Nikita, and A. Marioli. A four-dimensional simulation model of tumour response to radiotherapy in vivo: parametric validation considering radiosensitivity, genetic profile and fractionation. *J. Theor. Biol.*, 230:1–20, 2004.

W. Düchting, W. Ulmer, R. Lehrig, T. Ginsberg, and E. Dedeleit. Computer simulation and modelling of tumor spheroid growth and their relevance for optimization of fractionated radiotherapy. *Strahlenther Onkol.*, 168:354–360, 1992.

W. Düchting, T. Ginsberg, and W. Ulmer. Modeling of radiogenic responses induced by fractionated irradiation in malignant and normal tissue. *Stem Cells.*, 13 Suppl 1:301–306, 1995.

C.R. Dulaney, D.O. Osula, E. Yang, and S. Rais-Bahrami. Quality of life outcomes from a dose-per-fraction escalation trial of hypofractionation in prostate cancer. *Prostate Cancer*, 2016:ID: 4897515, 2016.

J. F. Fowler. The linear-quadratic formula and progress in fractionated radiotherapy. *Br. J. Radiol.*, 62:679–694, 1989.

J. F. Fowler. Biological factors influencing optimum fractionation in radiation therapy. *Acta Oncol.*, 40:712–717, 2001.

J. F. Fowler. Is there an optimum overall time for head and neck radiotherapy? A review, with new modelling. *Clin. Oncol.*, 19:8–22, 2007.

J. F. Fowler. Optimum overall times II: Extended modelling for head and neck radiotherapy. *Clin. Oncol.*, 20:113–126, 2008.

J. F. Fowler. 21 years of Biologically Effective Dose. *Br. J. Radiol.*, 83:554–568, 2010.

J. F. Fowler. Practical time-dose evaluations, or how to stop worrying and learn to love linear quadratics. In S. H. Levitt, J. A. Purdy, C. A. Perez, and P. Poortmans, editors, *Technical Basis of Radiation Therapy*, pages 3–50. Springer-Verlag, Berlin, 2012.

J. F. Fowler, P. M. Harari, F. Leborgne, and J. H. Leborgne. Acute radiation reactions in oral and pharyngeal mucosa: tolerable levels in altered fractionation schedules. *Radiother. Oncol.*, 69:161–168, 2003a.

J. F. Fowler, M. A. Ritter, R. J. Chappel, and D. J. Brenner. What hypofractionated protocols should be tested for prostate cancer? *Int. J. Radiat. Oncol. Biol. Phys.*, 56:1093–1104, 2003b.

J. F. Fowler, I. Toma-Dasu, and A. Dasu. Is the α/β ratio for prostate tumours really low and does it vary with the level of risk at diagnosis? *Anticancer Research*, 33:1009–1012, 2013.

M. Gao, N.A. Mayr, Z. Huang, H. Zhang, and J.Z. Wang. When tumor repopulation starts? the onset time of prostate cancer during radiation therapy. *Acta Oncol.*, 49:1269–1275, 2010.

E.C. Halperin, D.E. Wazer, C.A. Perez, and L.W. Brady. *Perez and Brady' s Principles and Practice of Radiation Oncology*. Lippincott Williams Wilkins, 2013.

W. M. Harriss-Philips, E. Bezak, and A. Potter. Stochastic predictions of cell kill during stereotactic ablative radiation therapy: Do hypoxia and reoxygenation really matter? *Int. J. Radiat. Oncol. Biol. Phys.*, 95:1290–1297, 2016.

L. R. Hlatky, P. Hahnfeldt, and R. K. Sachs. Influence of time-dependent stochastic heterogeneity on the radiation response of a cell population. *Math. Biosci.*, 122:201–220, 1994.

B. Jones and R. G. Dale. Mathematical models of tumour and normal tissue response. *Acta Oncol.*, 38:883–893, 1999.

C.R. King, J.D. Brooks, H. Gill, and J.C.Jr. Presti. Long-term outcomes from a prospective trial of stereotactic body radiotherapy for low-risk prostate cancer. *Int. J. Radiat. Oncol. Biol. Phys.*, 82:877–882, 2012.

J. P. Kirkpatrick, J. J. Meyer, and L. B. Marks. The linear-quadratric model is inappropriate to model high dose per fraction effects in radiosurgery. *Semin. Radiat. Oncol.*, 18:240–243, 2008.

J. P. Kirkpatrick, D. J. Brenner, and C. G. Orton. Point/counterpoint. the linear-quadratric model is inappropriate to model high dose per fraction effects in radiosurgery. *Med. Phys.*, 36: 3381–3384, 2009.

B.F. Koontz, A. Bossi, C. Cozzarini, T. Wiegel, and A. D'Amico. A systematic review of hypofractionation for primary management of prostate cancer. *Europ. Urol.*, 68:683–691, 2015.

U. Ledzewicz and H. Schättler. Multi-input optimal control problems for combined tumor antiangiogenic and radiotherapy treatments. *Journal of Optimization Theory and Applications*, 153:195–224, 2012.

E. K. Lee, T. Fox, and I. Crocker. Simultaneous beam geometry and intensity map optimization in intensity-modulated radiation therapy. *Int. J. Radiat. Oncol. Biol. Phys.*, 64:301–320, 2006.

R. Li, P. Keall, and L. Xing. Linac-Based image guided Intensity Modulated Radiation Therapy. In S. H. Levitt, J. A. Purdy, C. A. Perez, and P. Poortmans, editors, *Technical Basis of Radiation Therapy*, pages 275–312. Springer-Verlag, Berlin, 2012.

C. C. Ling, L. E. Gerweck, M. Zaider, and E. Yorke. Dose-rate effects in external beam radiotherapy redux. *Radiother. Oncol.*, 95:261–268, 2010.

W. Lu, M. Chen, Q. Chen, K. Ruchala, and G. Olivera. Adaptive fractionation therapy: I. Basic concept and strategy. *Phys. Med. Biol.*, 53:5495–5511, 2008a.

W. Lu, M. Chen, Q. Chen, K. Ruchala, and G. Olivera. Adaptive fractionation therapy: II. Biological effective dose. *Phys. Med. Biol.*, 53:5513–5525, 2008b.

G. Macchia, G. Ferrandina, F. Deodato, V. Ruggieri, M. Massaccesi, V. Salutari, V. Valentini, N. Cellini, G. Scambia, and A. G. Morganti. Concomitant boost dose escalation plus large-field preoperative chemoradiation in locally advanced carcinoma of the uterine cervix: Results of a phase i study (LARA-CC-1). *Gyn. Onc.*, 118:128–133, 2010.

J.M. Martin, T. Rosewall, A. Bayley, R. Bristow, P. Chung, J. Crook, M. Gospodarowicz, M. McLean, C. Menard, M. Milosevic, P. Warde, and C. Catton. Phase ii trial of hypofractionated image-guided intensity-modulated radiotherapy for localized prostate adenocarcinoma. *Int. J. Radiat. Oncol. Biol. Phys.*, 69:1084–1089, 2007.

C. Menkarios, E. Vigneault, N. Brochet, D. H. Nguyen, J. P. Bahary, M. Jolicoeur, M. C. Beauchemin, H. Villeneuve, T. Van Nguyen, B. Fortin, and C. Lambert. Toxicity report of once weekly radiation therapy for low-risk prostate adenocarcinoma: preliminary results of a phase I/II trial. *Radiat. Oncol.*, 6, 2011. article 112.

R. Miralbell, Roberts S.A., E. Zubizarreta, and J.H. Hendry. Dose-fractionation sensitivity of prostate cancer deduced from radiotherapy outcomes of 5969 patients in seven international institutional datasets: α/β=1.4 (0.9-2.2) Gy. *Int. J. Radiat. Oncol. Biol. Phys.*, 82:e17–e24, 2012.

M. Mizuta, S. Takao, H. Date, N. Kishimoto, K. L. Sutherland, R. Onimaru, and H. Shirato. A mathematical study to select fractionation regimen based on physical dose distribution and the linear-quadratic model. *Int. J. Radiat. Oncol. Biol. Phys.*, 84:829–833, 2012.

A.E. Nahum, B. Movsas, E.M. Horwitz, C.C. Stobbe, and J.D. Chapman. Incorporating clinical measurements of hypoxia into tumor local control modeling of prostate cancer: Implications for the α/β ratio. *Int. J. Radiat. Oncol. Biol. Phys.*, 57:391–401, 2003.

M. Oliveira, N.J. Teixeira, and L. Fernandes. What do we know about the α/β for prostate cancer? *Med. Phys.*, 39:3189–3201, 2012.

S. F. C. O'Rourke, H. McAneney, and T. Hillen. Linear quadratic and tumour control probability modelling in external beam radiotherapy. *J. Math. Biol.*, 58:799–817, 2009.

D. A. Pierre. *Optimization Theory with Applications.* John Wiley & Sons, New York, 1969.

C. Proust-Lima, J.M. Taylor, S. Secher, H. Sandler, L. Kestin, T. Pickles, K. Bae, R. Allison, and S. Williams. Confirmation of a low α/β ratio for prostate cancer treated by external beam radiation therapy alone using a post-treatment repeated-measures model for PSA dynamics. *Int. J. Radiat. Oncol. Biol. Phys.*, 79:195–201, 2011.

X. S. Qi, C. J. Schultz, and X. A. Li. An estimation of radiobiologic parameters from clinical outcomes for radiation treatment planning of brain tumor. *Int. J. Radiation Oncology Biol. Phys.*, 64:1570–1580, 2006.

X. S. Qi, J. White, and X. A. Li. Is α/β for breast cancer really low? *Radiother. Oncol.*, 100: 282–288, 2011.

B. Ribba, T. Colin, and S. Schnell. A multiscale mathematical model of cancer, and its use in analyzing irradiation therapies. *Theor. Biol. Med. Model.*, 3:7, 2006. doi:10.1186/1742-4682-3-7.

M. Ritter, J. Forman, P. Kupelian, C. Lawton, and D. Petereit. Hypofractionation for prostate cancer. *Cancer J.*, 15:1–6, 2009.

F. Saberian, A. Ghate, and M. Kim. Optimal fractionation in radiotherapy with multiple normal tissues. *Math. Med. Biol.*, 32, 2015. doi:10.1093/imammb/dqv015.

C. I. Tang, D. A. Loblaw, P. Cheung, L. Holden, G. Morton, P. S. Basran, R. Tirona, M. Cardoso, G. Pang, S. Gardner, and A. Cesta. Phase I/II study of a five-fraction hypofractionated accelerated radiotherapy treatment for low-risk localised prostate cancer: early results of pHART3. *Clin. Oncol. (R. Coll. Radiol.)*, 20:729–737, 2008.

H. D. Thames. An 'incomplete-repair' model for survival after fractionated and continuous irradiations. *Int. J. Radiat. Biol.*, 47:319–339, 1985.

H. D. Thames, S.M. Bentzen, I. Turesson, M. Overgaard, and W. Van den Bogaert. Time-dose factors in radiotherapy: a review of the human data. *Radiother. Oncol.*, 19:219–235, 1990.

J.Z. Wang and X. A. Li. Impact of tumor repopulation on radiotherapy planning. *Int. J. Radiat. Oncol. Biol. Phys.*, 61:220–227, 2005.

J.Z. Wang, M. Guerrero, and X. A. Li. How low is the alpha/beta ratio for prostate cancer? *Int. J. Radiat. Oncol. Biol. Phys.*, 55:194–203, 2003.

T.J. Whelan, D.H. Kim, and J. Sussman. Clinical experience using hypofractionated radiation schedules in breast cancer. *Semin. Radiat. Oncol.*, 18:257–264, 2008.

C. S. Wong and R. P. Hill. Experimental radiotherapy. In I. F. Tannock and R. P. Hill, editors, *The Basic Science of Oncology.*, pages 322–349. McGraw-Hill, New York, 1998.

Y. Yang and L. Xing. Optimization of radiotherapy dose-time fractionation with consideration of tumor specific biology. *Med. Phys.*, 32:3666–3677, 2005.

J1. Yarnold, A. Ashton, J. Bliss, J. Homewood, C. Harper, J. Hanson, J. Haviland, S. Bentzen, and R. Owen. Fractionation sensitivity and dose response of late adverse effects in the breast after radiotherapy for early breast cancer: long-term results of a randomised trial. *Radiother. Oncol.*, 75:9–17, 2005.

Appendix A. KKT necessary and admissibility conditions of optimality for Problem 2.2

In this section we provide the set of Karush-Kuhn-Tucker conditions for Problem 2.2 used to derive some results characterizing the structure of the optimal solutions. Because of the non-convexity of Problem 2.2, we can only use the optimality necessary conditions provided by the Karush-Kuhn-Tucker Theorem (Pierre, 1969). The existence of optimal solutions is guaranteed by the Weierstrass theorem.

Recalling that n is a fixed integer in Problem 2.2, let us write the Lagrangian function associated to Problem 2.2 as

$$L(d, \lambda_0, \eta_e, \eta_l, \eta, \mu) = \lambda_0 J_n(d) + \eta_e g_e(n, d) + \eta_l g_l(n, d) - \sum_{k=1}^{n} \eta_k d_k + \sum_{k=1}^{n} \mu_k (d_k - d_M)\,,$$

where λ_0, η_e, η_l are scalar multipliers and η, μ are n-dimensional vectors with components $\eta_k, \mu_k, k = 1, \ldots, n$, respectively. Introducing the notations

$$\delta(\lambda_0, \eta_e, \eta_l) \;=\; -\lambda_0 \rho + \eta_e \rho_e + \eta_l \rho_l\,, \qquad \sigma(\lambda_0, \eta_e, \eta_l) \;=\; 2(-\lambda_0 + \eta_e + \eta_l)\,, \tag{A.1}$$

the necessary and admissibility conditions are

$$\frac{\partial L}{\partial d_k} \;=\; \delta(\lambda_0, \eta_e, \eta_l) + \sigma(\lambda_0, \eta_e, \eta_l) d_k - \eta_k + \mu_k = 0\,,\; k = 1, \ldots, n\,, \tag{A.2}$$

$$\eta_k d_k = 0\,, \quad k = 1, \ldots, n\,, \tag{A.3}$$

$$\mu_k (d_k - d_M) = 0\,, \quad k = 1, \ldots, n\,, \tag{A.4}$$

$$\eta_e g_e(d) = 0\,, \tag{A.5}$$

$$\eta_l g_l(d) = 0\,, \tag{A.6}$$

$$g_e(d) \le 0\,, \quad g_l(d) \le 0\,, \tag{A.7}$$

$$0 \le d_k \le d_M\,, \quad k = 1, \ldots, n\,, \tag{A.8}$$

$$\lambda_0, \eta_e, \eta_l, \eta_k, \mu_k \ge 0\,, \quad k = 1, \ldots, n\,, \tag{A.9}$$

with λ_0, η_e, η_l, η_k, μ_k, $k = 1, \ldots, n$, not simultaneously equal to zero.

Let us now examine the subsystem made of equations (A.2), (A.3) and (A.4) considering as the only unknowns d, η, μ, and assuming λ_0, η_e, η_l fixed. Fixing the triple λ_0, η_e, η_l, the quantities δ and σ in (A.1) become fixed coefficients of equations (A.2). In such a way, it is easy to derive some structural properties of the optimal solutions in terms of δ and σ.

Theorem 5.1. *For any fixed integer n, Problem 2.2 admits two sets of solutions: "structured" and "non-structured". The set of structured solutions is associated to values of λ_0, η_e, η_l such that $\sigma \neq 0$ and it consists at most of 3^n structures (including the trivial vector $d = 0$) that can be grouped into $(n+1)(n+2)/2$ mutually exclusive classes. Structures in each class are characterized by the number of doses equal to zero, d_M and $A \in (0, d_M)$, with*

$$A = -\frac{\delta}{\sigma}\,, \tag{A.10}$$

independently of the dose positions. Having the same value of the cost function $J_n(d)$, all the structures of the same class are equivalent. All the classes are summarized by the set of representative vectors $\{d(i,j),\, i,j=0,\ldots,n,\, 0\le i+j\le n\}$, where i denotes the number of doses equal to A and j the number of doses equal to d_M. Being the intermediate dose A dependent on the class, $A(i,j)$ denotes its value for the structure $d(i,j)$, $i\neq 0$.

The set of non-structured candidates is associated to values of the multipliers λ_0, η_e, η_l such that $\sigma=\delta=0$, and consequently $\eta=\mu=0$, making Eqs. (A.2) *identically satisfied.*

Proof. Let us multiply each equation $\dfrac{\partial L}{\partial d_k}=0$ in (A.2) by $d_k\,(d_k-d_M)$. In view of (A.3) and (A.4), we obtain

$$d_k\,(d_k-d_M)(\delta+\sigma d_k)=0\,,\ k=1,\ldots,n\,,$$

and, for values of the multipliers λ_0, η_e, η_l such that $\sigma\neq 0$, we get three values for d_k:

$$d_k=0\,,\qquad d_k=d_M\,,\qquad d_k=-\frac{\delta}{\sigma}=A\,. \tag{A.11}$$

For $A\in(0,d_M)$, the values (A.11) are distinct and their 3^n dispositions with repetition in a vector $d\in R^n$ give all the possible structured solutions. As vectors containing the same number of A and d_M are indistinguishable with respect to J_n, i.e. they are equivalent, the vectors can be grouped into $(n+1)(n+2)/2$ mutually exclusive classes of equivalent structures, in which a single structure can be chosen as a representative.

Let us now reconsider the original system (A.2)–(A.4) supposing that the fixed values of the multipliers λ_0, η_e, η_l are such that $\sigma=0$. If $\delta\neq 0$ it can be verified that the solutions are $d(0,0)$ and $d(0,n)$, already present among structures. If instead $\delta=0$, Eqs. (A.2)–(A.4) imply $\eta_k=\mu_k=0$, $k=1,\ldots,n$, and the system is identically satisfied, providing no information about the value of d_k or the structure of d. Therefore, when $\sigma=\delta=0$ the system of necessary conditions admits a set of "non-structured" solutions associated to multipliers $\eta=\mu=0$ with dose values defined only by constraints (A.5) and (A.6). ∎

Appendix B. Minimum value of the maximal entry of n-dimensional vectors with constant sum of the entries and of the squared entries

Recalling that $S>0$, $v\in[1,n]$ (see their definitions in Eqs. (25), (19)) and considering the ordering $d_n\ge d_{n-1}\ge\ldots\ge d_2\ge d_1\ge 0$, among the entries of the vector d, we can formulate the following optimization problem.

Problem 5.2. *Minimize the function:*

$$\tilde{J}(d)=d_n, \tag{B.1}$$

on the admissible set:

$$\tilde{D}=\{d\in R^n|\quad \sum_{k=1}^{n}d_k=S\,,\ \sum_{k=1}^{n}d_k^2=\frac{S^2}{v}\,,\ \ d_n\ge d_{n-1}\ge\ldots\ge d_2\ge d_1\ge 0\,,\ \ v\in[1,n]\}\,. \tag{B.2}$$

Firstly, we note that $\tilde{D}$ is non-empty as $v\in[1\,,n]$. Secondly, Problem 5.2 certainly admits an optimal solution as the admissible set (B.2) is compact and the cost function (B.1) is continuous

on it (Weierstrass theorem (Pierre, 1969)). Moreover, it is evident that the Problem 5.2 is not convex so that we can only use the optimal necessary conditions provided by the Kuhn Tucker Theorem (Pierre, 1969). The Lagrangian function associated to the problem is

$$\tilde{L}(d,\lambda_0,\lambda_s,\lambda_q,\eta)=\lambda_0 d_n+\lambda_s\left(\sum_{k=1}^{n} d_k-S\right)+\lambda_q\left(\sum_{k=1}^{n} d_k^2-\frac{S^2}{v}\right)-\eta_1 d_1+\sum_{k=1}^{n-1}\eta_{k+1}\left(d_k-d_{k+1}\right), \quad \text{(B.3)}$$

where $\lambda_0\,,\lambda_s\,,\lambda_q$ are scalar multipliers and η is the n-dimensional vector of multipliers η_k, $k=1,\ldots,n$, related to the inequality constraints.

Let us now write the necessary and admissibility conditions

$$\frac{\partial\tilde{L}}{\partial d_k} = \lambda_s+2\lambda_q d_k-\eta_k+\eta_{k+1}=0\,, \qquad k=1,\ldots,n-1\,, \quad \text{(B.4)}$$

$$\frac{\partial\tilde{L}}{\partial d_n} = \lambda_0+\lambda_s+2\lambda_q d_n-\eta_n=0\,, \quad \text{(B.5)}$$

$$\eta_1 d_1 = 0\,, \quad \text{(B.6)}$$

$$\eta_k(d_{k-1}-d_k) = 0\,, \qquad k=2\,,\ldots,n\,, \quad \text{(B.7)}$$

$$\sum_{k=1}^{n} d_k = S\,, \quad \text{(B.8)}$$

$$\sum_{k=1}^{n} d_k^2 = \frac{S^2}{v}\,, \quad \text{(B.9)}$$

$$d_k\geq d_{k-1} \geq 0\,, \qquad k=2\,,\ldots\,,n\,, \quad \text{(B.10)}$$

$$\eta_k \geq 0\,, \qquad k=1\,,\ldots\,,n\,, \quad \text{(B.11)}$$

$$\lambda_0 \geq 0\,, \quad \text{(B.12)}$$

with $\lambda_0\,,\lambda_s\,,\lambda_q\,,\eta$ never simultaneously equal to zero. The vectors d, and the related multipliers $\lambda_0\,,\lambda_s\,,\lambda_q\,,\eta$ that satisfy system (B.4)–(B.12), are the extremals of Problem 5.2, that is all the possible candidates to the optimal solution.

Let us multiply each equation $\dfrac{\partial\tilde{L}}{\partial d_k}=0$ in (B.4)–(B.5) by the corresponding $d_k\,,\ k=1\,,\ldots\,,n$, and let us add together the n equations so obtained, taking also into account Eqs. (B.6)–(B.9). We get the relation

$$\lambda_0 d_n+\lambda_s S+2\lambda_q\frac{S^2}{v}=0\,, \quad \text{(B.13)}$$

which constitutes a constraint on the values of the multipliers $\lambda_0\,,\lambda_s\,,\lambda_q$. Exploiting Eq. (B.13), together with Eqs. (B.4)–(B.7) and (B.10)–(B.12), it is possible to characterize the structure of the solution pairs $d\,,\eta$. The main emerging property is that the vector d (associated to a specific triple $\lambda_0\,,\lambda_s\,,\lambda_q$ and to a specific multiplier vector η) can contain at most two different positive entries (the details of this analysis are reported in the Technical Report by Conte et al. (2015)). Denoting these entries by x, y, with $y>x>0$, and recalling the assumed ordering $d_n\geq d_{n-1}\geq\ldots\geq d_2\geq d_1\geq 0$, all the solution vectors d can only have two possible structures characterized by: i) the last j entries equal to a positive value, y, and (possibly) the first $n-j$

entries equal to zero; ii) the last j entries equal to y, the preceding i entries equal to x and (possibly) the first $n-i-j$ entries equal to zero. When d contains only positive entries equal to y, Eqs. (B.8) , (B.9) lead to the system

$$\begin{cases} jy = S\,, \\ jy^2 = \dfrac{S^2}{v}\,, \end{cases} \tag{B.14}$$

which admits the real positive solution $y = S/v$ only for v integer and equal to j. Conversely, when d contains two different positive values x, y, in order to satisfy the constraints (B.8) , (B.9), it is necessary to solve the system

$$\begin{cases} ix + jy = S\,, \\ ix^2 + jy^2 = \dfrac{S^2}{v}\,. \end{cases} \tag{B.15}$$

As it must be $y > x > 0$, system (B.15) admits a unique real positive solution

$$x = R^-_{j,i}\,, \tag{B.16}$$

$$y = R^+_{i,j}\,, \tag{B.17}$$

for each pair i, j such that $j < v < i + j$, where

$$R^-_{j,i} = \frac{S}{i+j}\left(1 - \sqrt{\frac{j(i+j-v)}{vi}}\right)\,, \tag{B.18}$$

and

$$R^+_{i,j} = \frac{S}{i+j}\left(1 + \sqrt{\frac{i(i+j-v)}{vj}}\right)\,. \tag{B.19}$$

Indeed, it is easy to verify that the quantities $R^-_{j,i}$, $R^+_{i,j}$ are real and positive, with $R^+_{i,j} > R^-_{j,i}$, if and only if $j < v < i + j$.

As it is proved in Conte et al. (2015), the set of structured extremals of Problem 5.2 depends on the value of v. Table 13 summarizes the extremals of the optimization problem for each subinterval of v in $[1, n]$. We note that, when $v = [v]$, if $j = [v]$ it is $R^-_{[v],i} = 0$, $R^+_{i,[v]} = S/[v]$, so that extremals coming from system (B.15) with $j = [v]$ coincide with the vector having $[v]$ entries equal to $S/[v]$ and $n - [v]$ zeroes, that is the solution of system (B.14). In order to actually determine the optimal solution in each interval of v reported in Table 13, we need to evaluate the cost function $\tilde{J}$ in (B.1) for all the extremals of the interval itself, identifying the minimum among the selected structures. To this purpose we preliminary study the behaviour of $R^+_{i,j}$ defined in (B.19) keeping fixed the sum $s = i + j$ but letting i vary, and then fixing the index j but letting s vary. Rewriting $R^+_{i,j}$ as a function $R^+(i, s-i)$ and considering i, s as positive continuous variables, we have

$$\frac{\partial R^+(i, s-i)}{\partial i} = \frac{S}{2}\sqrt{\frac{s-v}{vi(s-i)^3}}\,, \tag{B.20}$$

which is strictly positive since $v < s$. On the other hand, rewriting $R^+_{i,j}$ as a function $R^+(s-j, j)$ and considering s, j as positive continuous variables, we have

$$\frac{\partial R^+(s-j, j)}{\partial s} = \frac{S\left(\sqrt{v(s-j)} - \sqrt{j(s-v)}\right)^2}{2s^2\sqrt{vj(s-j)(s-v)}}\,, \tag{B.21}$$

which is strictly positive as $v > j$. Therefore, for a fixed sum $i + j$, $R^+_{i,j}$ increases as i increases, while for a fixed j, $R^+_{i,j}$ increases as the sum $i + j$ increases.

Taking into account (B.20) and (B.21), it is easy to determine, in each interval of v, the optimal solutions of Problem (5.2) which are listed Table 14.

In conclusion, the optimum of Problem (5.2) is the vector d^R having the last $[v]$ entries equal to $R_{1,[v]} \triangleq R^+_{1,[v]}$ (equal to S/v if $v = [v]$), one entry equal to $R^-_{[v],1} = S - [v]R_{1[v]}$ provided $v < n$ (equal to zero if $v = [v]$) and the remaining $n - [v] - 1$ entries equal to zero provided $v < n - 1$.

Table 13: Extremals of Problem 5.2 classified on the basis of v sub-intervals.

$\boldsymbol{v}$	$\boldsymbol{d}$
$[1,2)$	$(0 \;\; 0 \;\; \ldots \;\; 0 \;\; 0 \;\; R^-_{1,1} \;\; R^+_{1,1})$ $(0 \;\; 0 \;\; \ldots \;\; 0 \;\; R^-_{1,2} \;\; R^-_{1,2} \;\; R^+_{2,1})$ $\vdots$ $(0 \;\; R^-_{1,n-2} \;\; \ldots \;\; R^-_{1,n-2} \;\; R^-_{1,n-2} \;\; R^+_{n-2,1})$ $(R^-_{1,n-1} \;\; R^-_{1,n-1} \;\; \ldots \;\; R^-_{1,n-1} \;\; R^-_{1,n-1} \;\; R^+_{n-1,1})$
$[2,3)$	$(0 \;\; 0 \;\; \ldots \;\; 0 \;\; R^-_{1,2} \;\; R^-_{1,2} \;\; R^+_{2,1})$ $(0 \;\; 0 \;\; \ldots \;\; 0 \;\; R^-_{2,1} \;\; R^+_{1,2} \;\; R^+_{1,2})$ $(0 \;\; 0 \;\; \ldots \;\; 0 \;\; R^-_{1,3} \;\; R^-_{1,3} \;\; R^-_{1,3} \;\; R^+_{3,1})$ $(0 \;\; 0 \;\; \ldots \;\; 0 \;\; R^-_{2,2} \;\; R^-_{2,2} \;\; R^+_{2,2} \;\; R^+_{2,2})$ $\vdots$ $(R^-_{1,n-1} \;\; R^-_{1,n-1} \;\; R^-_{1,n-1} \;\; R^-_{1,n-1} \;\; R^+_{n-1,1})$ $(R^-_{2,n-2} \;\; R^-_{2,n-2} \;\; R^-_{2,n-2} \;\; R^+_{n-2,2} \;\; R^+_{n-2,2})$
$\vdots$	$\vdots$
$[n-2,n-1)$	$(0 \;\; R^-_{1,n-2} \;\; \ldots \;\; R^-_{1,n-2} \;\; R^-_{1,n-2} \;\; R^+_{n-2,1})$ $(0 \;\; R^-_{2,n-3} \;\; \ldots \;\; R^-_{2,n-3} \;\; R^+_{n-3,2} \;\; R^+_{n-3,2})$ $\vdots$ $(0 \;\; R^-_{n-2,1} \;\; R^+_{1,n-2} \;\; \ldots \;\; R^+_{1,n-2} \;\; R^+_{1,n-2})$ $(R^-_{1,n-1} \;\; R^-_{1,n-1} \;\; \ldots \;\; R^-_{1,n-1} \;\; R^-_{1,n-1} \;\; R^+_{n-1,1})$ $(R^-_{2,n-2} \;\; R^-_{2,n-2} \;\; \ldots \;\; R^-_{2,n-2} \;\; R^+_{n-2,2} \;\; R^+_{n-2,2})$ $\vdots$ $(R^-_{n-2,2} \;\; R^-_{n-2,2} \;\; R^+_{2,n-2} \;\; \ldots \;\; R^+_{2,n-2} \;\; R^+_{2,n-2})$
$[n-1,n)$	$(R^-_{1,n-1} \;\; R^-_{1,n-1} \;\; \ldots \;\; R^-_{1,n-1} \;\; R^-_{1,n-1} \;\; R^+_{n-1,1})$ $(R^-_{2,n-2} \;\; R^-_{2,n-2} \;\; \ldots \;\; R^-_{2,n-2} \;\; R^+_{n-2,2} \;\; R^+_{n-2,2})$ $(R^-_{3,n-3} \;\; \ldots \;\; R^-_{3,n-3} \;\; R^+_{n-3,3} \;\; R^+_{n-3,3} \;\; R^+_{n-3,3})$ $\vdots$ $(R^-_{n-1,1} \;\; R^+_{1,n-1} \;\; \ldots \;\; R^+_{1,n-1} \;\; R^+_{1,n-1} \;\; R^+_{1,n-1})$
n	$(S/n \;\; S/n \;\; \ldots \;\; S/n \;\; S/n \;\; S/n)$

Table 14: Optimal solution of Problem 5.2 as a function of v. When $v = [v]$ it is $R^+_{1,[v]} = S/v$, $R^-_{[v],1} = 0$.

$\boldsymbol{v}$	$\boldsymbol{d}$
$[1,2)$	$(0 \quad \dots \quad 0 \quad 0 \quad R^-_{1,1} \quad R^+_{1,1})$
$[2,3)$	$(0 \quad \dots \quad 0 \quad R^-_{2,1} \quad R^+_{1,2} \quad R^+_{1,2})$
$\vdots$	$\vdots$
$[n-2,n-1)$	$(0 \quad R^-_{n-2,1} \quad R^+_{1,n-2} \quad \dots \quad R^+_{1,n-2} \quad R^+_{1,n-2})$
$[n-1,n)$	$(R^-_{n-1,1} \quad R^+_{1,n-1} \quad R^+_{1,n-1} \quad \dots \quad R^+_{1,n-1} \quad R^+_{1,n-1})$
n	$(S/n \quad S/n \quad \dots \quad S/n \quad S/n \quad S/n)$